Journal of Medicinal Chemistry

Article

The Identification of (*R*)-(2-chloro-3-(trifluoromethyl)phenyl) (1-(5-fluoropyridin-2-yl)-4-methyl-6,7-dihydro-1H-imidazo[4,5-c]pyridin-5(4H)-yl)methanone (JNJ 54166060), a small molecule antagonist of the P2X7 receptor

Devin Maun Swanson, Brad M. Savall, Kevin J Coe, Freddy Schoetens, Tatiana Koudriakova, Judith Skaptason, Jessica Wall, Jason C. Rech, Xiahou Deng, Meri De Angelis, Anita Everson, Brian Lord, Qi Wang, Hong Ao, Brian Scott, Kia Sepassi, Timothy W Lovenberg, Nicholas I. Carruthers, Anindya Bhattacharya, and Michael A Letavic

J. Med. Chem., **Just Accepted Manuscript** • DOI: 10.1021/acs.jmedchem.6b00989 • Publication Date (Web): 22 Aug 2016

Just Accepted

ACS Publications

Journal of Medicinal Chemistry is published by the American Chemical Society. 1155 Sixteenth Street N.W., Washington, DC 20036

The Identification of (*R*)-(2-chloro-3-(trifluoromethyl)phenyl)(1-(5-fluoropyridin-2-yl)-4-methyl-6,7-dihydro-1H-imidazo[4,5-c]pyridin-5(4H)-yl)methanone (JNJ 54166060), a small molecule antagonist of the P2X7 receptor

Devin M. Swanson,[†,*] Brad M. Savall,[†] Kevin J. Coe,[†] Freddy Schoetens,[†] Tatiana Koudriakova,[†] Judith Skaptason,[†] Jessica Wall,[†] Jason Rech,[†] Xiahou Deng,[†] Meri De Angelis,[‡] Anita Everson,[†] Brian Lord,[†] Qi Wang,[†] Hong Ao,[†] Brian Scott,[†] Kia Sepassi,[†] Timothy W. Lovenberg,[†] Nicholas I. Carruthers,[†] Anindya Bhattacharya,[†] and Michael A. Letavic[†]

[†]*Janssen Pharmaceutical Research & Development, LLC, 3210 Merryfield Row, San Diego, CA, 92121 USA*

[‡]*Janssen Research & Development, Discovery Sciences, A Division of Janssen-Cilag, Jarama 75, 45007 Toledo, Spain*

Abstract

The synthesis and SAR of a series of 4,5,6,7-tetrahydro-imidazo[4,5-c]pyridine P2X7 antagonists are described. Addressing P2X7 affinity and liver microsomal stability issues encountered with this template afforded methyl substituted 4,5,6,7-tetrahydro-imidazo[4,5-c]pyridines ultimately leading to the identification of **1** (JNJ 54166060). **1** is a potent P2X7 antagonist with an ED_{50} = 2.3 mg/kg in rat, high oral bioavailability and low-moderate clearance in pre-clinical species, acceptable safety margins in rat, and a predicted human dose of 120 mg QD. Additionally, **1** possesses a unique CYP profile and was found to be a regioselective inhibitor of midazolam CYP3A metabolism.

Introduction

The P2X7 receptor is an ATP gated, purinergic ion channel that controls the release of pro inflammatory cytokines (IL-1β, IL-18) in both the periphery and the central nervous system.[1] The P2X7 receptor belongs to the P2X family of ionotropic receptors and is expressed peripherally in hematopoietic cells such as lymphocytes, monocytes, and macrophages and centrally in microglia and astrocytes.[2] Of the seven subtypes, the P2X7 receptor possesses the lowest affinity for ATP, and thus under normal circumstances, the receptor remains silent. Upon increasing ATP concentrations the P2X7 receptor is activated and triggers a proinflammatory cascade via Ca^{2+} influx and subsequent IL-1β release.[3, 4] In addition to IL-1β signaling, P2X7 dependent release of glutamate, GABA, cathepsins, and chemokines have all been reported.[5-8]

The therapeutic importance of a P2X7 antagonist in humans is currently being assessed. At least two peripherally restricted compounds and one centrally penetrant compound have progressed into clinical trials. Pfizer reported their clinical candidate was tolerated but failed to show efficacy for the treatment of rheumatoid arthritis,[9] Astra Zeneca demonstrated efficacy in a proof of concept study in Crohn's disease,[10] and GSK published safety and tolerability data for GSK 1482160.[11] Our interest in the P2X7 receptor is focused on its central role in neuroinflammation, specifically the relationship between P2X7 antagonism, IL-1β suppression, and improvements in the symptoms of depression. Indeed several laboratories have shown that IL-1β mediates stress induced depression and anhedonia in mice while P2X7 knockouts are protected from depression like behavior.[12, 13]

Recently, GSK and our own laboratories have disclosed a series of 5,6,7,8-tetrahydro-[1,2,4]triazolo[4,3-a]pyrazines (1,2,4-triazolopyrazines), 4,5,6,7-tetrahydro-1H-[1,2,3]triazolo[4,5-c]pyridines (1,2,3-triazolopyridines), and related P2X7 antagonists with reasonable physiochemical properties and demonstrated target engagement in rat (**Figure 1**).[14-19]

The 1,2,4-triazolopyrazines (**2**,**4**,**5**) and 1,2,3-triazolopyridine (**3**) were shown to be potent human P2X7 antagonists that found utility as in vivo tool compounds for the program. The SAR from these series are summarized in a recent review.[20] As an extension of this work the 4,5,6,7-tetrahydro-1H-imidazo[4,5-c]pyridine (imidazopyridine) core was explored to advance novel P2X7 chemotypes with an improved ADME and safety profile. Herein we report the synthesis and SAR of the imidazopyridine series and the preclinical profile of **1** (JNJ 54166060).[21]

Figure 1. 1 (JNJ 54166060) and previously disclosed triazolopyrazines and triazolopyridines (**2-5**).

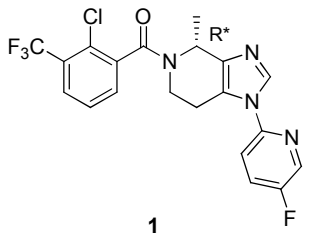

1
(JNJ 54166060)

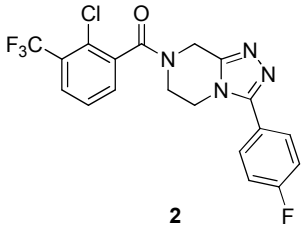

2
hP2X7 IC_{50} = 14 nM
rP2X7 IC_{50} = 6400 nM

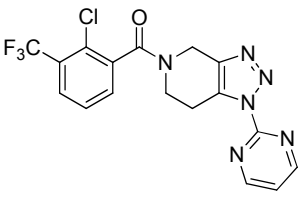

3
hP2X7 IC_{50} = 4 nM
rP2X7 IC_{50} = 7 nM

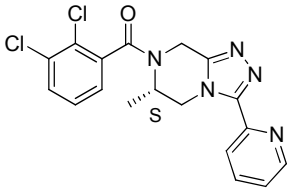

4
hP2X7 IC_{50} = 8 nM
rP2X7 IC_{50} = 8 nM

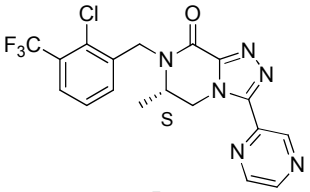

5
hP2X7 IC_{50} = 0.7 nM
rP2X7 IC_{50} = 79 nM

Results and Discussion

Our initial exploration into the imidazopyridine core involved first replacing the triazole in compounds **2** and **3** with a 1H-imidazole. Starting from commercially available 1H-imidazo[4,5-c]pyridine (**6**), we arylated the imidazole nitrogen using C-N coupling conditions to provide **7a** and **7b** as a 1:1 mixture of regioisomers which were separable by silica gel chromatography (**Scheme 1**).[22] From **7a** we reduced the imidazopyridine ring by forming an *N*-

alkylpyridinium ion with BnBr followed by $NaBH_4$ reduction to obtain **8**. Hydrogenolysis of the benzyl group and subsequent peptide coupling provided the final compounds, **10-17**.

Scheme 1. Synthesis of imidazopyridine compounds **10-17.**

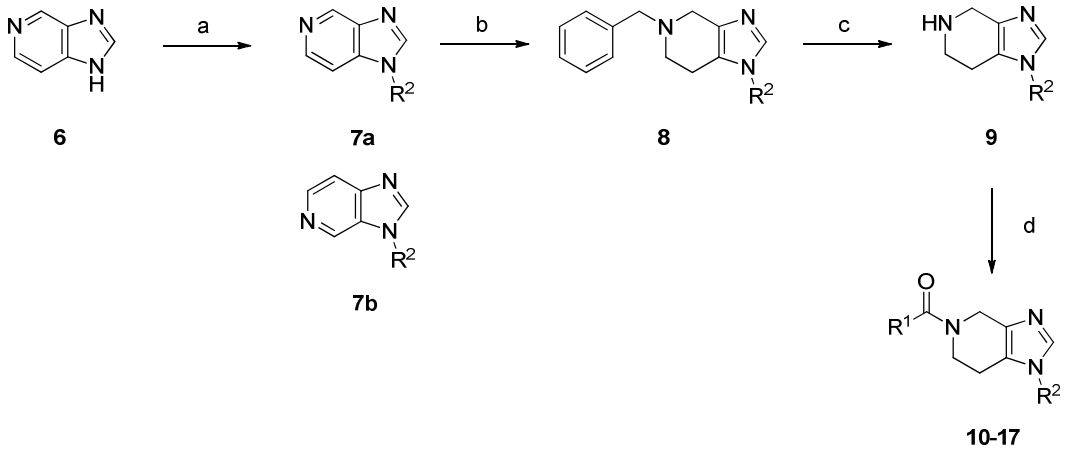

Reagents & Conditions: a) R^2-X, Cu_2O, 8-OH quinoline, Cs_2CO_3, DMSO, microwave, 1 h, 140 °C, 17-40% b) BnBr, $NaBH_4$, DCM, MeOH, rt, 68-87% c) H_2, EtOH, Pd/C, rt, 24 h, 75-83% d) R^1COOH, HATU, Et_3N, DMF, rt, 22-96%

Results from our initial analogs established that changing the core from a triazolopyridine to an imidazopyridine was tolerated with respect to hP2X7 affinity (**Table 1**). Thus compounds **10-17** all possessed a similar profile, with a hP2X7 IC_{50} < 100 nM and rP2X7 IC_{50} > 500 nM. Compound **12**, where R^1 = 2-Cl-3-CF_3 phenyl and R^2 = 2-pyridyl, provided the best combination of human and rat P2X7 affinity with a hP2X7 IC_{50} = 4 nM and a rP2X7 IC_{50} = 609 nM. The measured disconnect between human and rat P2X7 affinity has been previously observed in the triazolopyrazine and triazolopyridine templates as highlighted by compound **2**. Additionally, steep SAR was observed for the R^1 space where small changes to the 2-Cl-3-CF_3 phenyl substituent resulted in diminished hP2X7 affinity as seen with compounds **15-17**. Further profiling of these compounds identified microsomal stability as a liability for this template as measured extraction ratios (ERs) from human and rat liver microsomes (HLM/RLM) were all greater than 0.8 indicative of metabolic instability.

Table 1. Human and rat P2X7 IC_{50}s and microsomal data for compounds **10-17**.

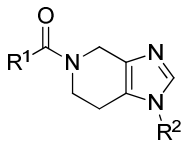

Compd	R^1	R^2	hP2X7 IC_{50} (nM)[a]	rP2X7 IC_{50} (nM)[b]	HLM/ RLM[c]
10	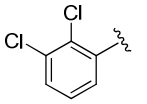		89	4006	0.93/>0.92
11	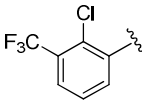		12	2909	0.94/0.89
12	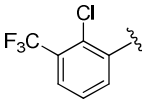		4	609	0.91/>0.92
13	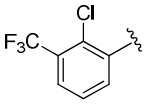		9	1782	0.9/0.87
14	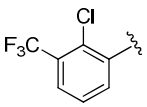	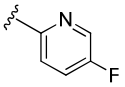	28	2476	0.84/0.87
15	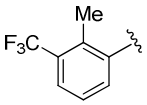	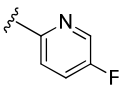	114	4872	--
16	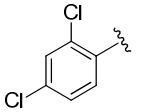	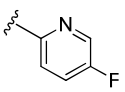	880	>10,000	--
17	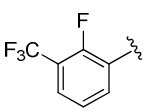	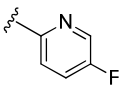	3538	>10,000	--

[a]All compounds were found to be P2X7 antagonists using a human peripheral blood monocyte (HPBMC) assay prior to testing in FLIPR for confirmation of activity and IC_{50} determination. The protocols for the HPBMC and FLIPR assays can be found in the Experimental Section. Human FLIPR pIC_{50} measured in a Ca^{2+} flux assay. [b]Rat FLIPR measured in a Ca^{2+} flux assay. [c]Stability in rat and human liver microsomes as measured by extraction

ratio(s). Primary assays run in triplicate with the mean value reported. Standard deviation in all cases was less than two-fold.

In the 1,2,4-triazolopyrazine series (**4**), methyl substitution on the core improved rat P2X7 affinity.[15] As such we wished to explore the impact of similar substitution on the imidazopyridine core and chose substitution on the 4- position due to synthetic accessibility. To synthesize these analogs we utilized the route shown in **Scheme 2** and kept the 2-chloro-3-trifluoromethylaryl group (R^1) constant due the SAR observed in **Table 1**. Here, we added a methyl Grignard to an *N*-acylpyridinium ion, formed by **7a** and an acid chloride (**18**), to affect a 1,2 addition which gave intermediate **19**.[23] This intermediate could then be reduced under hydrogenation conditions to provide the desired compounds, **20-27**, as racemic mixtures. Racemates of interest were then separated by chiral chromatography.

Scheme 2. Synthesis of imidazopyridine compounds **1** and **20-30.**

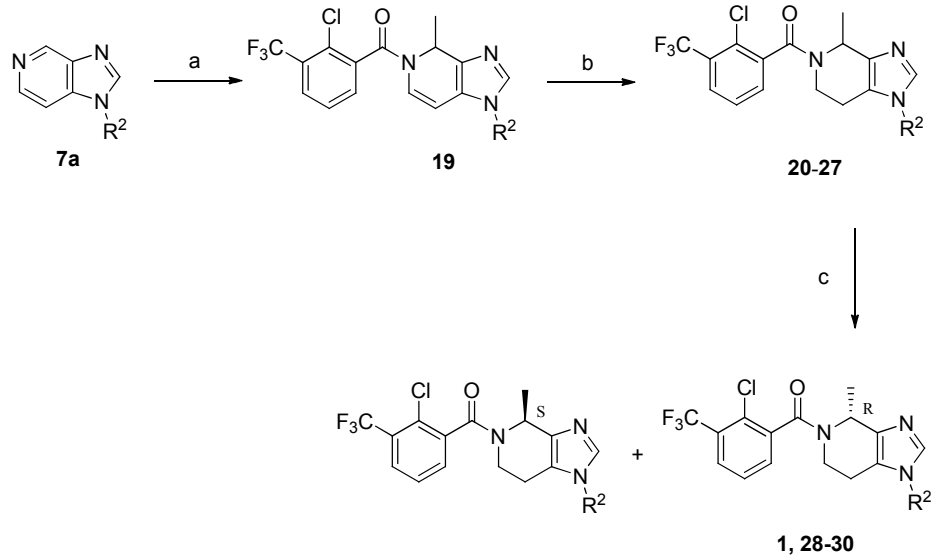

Reagents & Conditions: a) 2-Cl-3-CF3PhCOCl (**18**), MeMgBr, THF, rt, 3 h, 33-54% b) H_2, EtOH, Pd/C, 24 h, 20-62% c) SFC chiral chromatography, 40-42%

Shown in **Table 2** are the human and rat P2X7 IC_{50}s and microsomal stability data for compounds **20-27**. Compound **21** provided the first indication of increased microsomal stability within the series. Thus going from the unsubstituted phenyl (**20**) to a 4-F phenyl (**21**) saw

measurable improvement in stability with **21** possessing a HLM/RLM ER = 0.32/0.59. The 4-F pyrimidine derivative (**23**) and 4-F pyridine derivative (**27**) were also equally stable in vitro and both compounds possessed improved target affinity with a hP2X7 IC_{50} = 10 and 14 nM, respectively. Modest gains in rat affinity were observed with 4-Me substitution on the imidazopyridine core. Compounds **20**, **25**, and **27** were two to four fold more active at the rat P2X7 receptor over their des methyl equivalents (**11**, **12**, and **14**) and prompted additional investigation of the single enantiomers.

Table 2. Human and rat P2X7 IC_{50}s and liver microsomal stability data for compounds **20-27**.

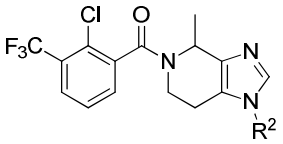

Compd	R^2	hP2X7 IC_{50} (nM)[a]	rP2X7 IC_{50} (nM)[b]	HLM/ RLM[c]
20	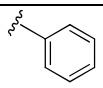	5	766	0.75/0.73
21	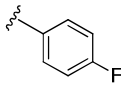	78	1182	0.32/0.59
22		30	113	0.79/0.80
23	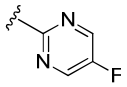	10	3828	<0.3/0.54
24		77	1225	0.77/0.84
25		34	295	0.74/0.89

26	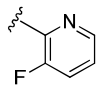	9	2319	0.81/0.81
27	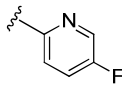	14	592	<0.3/0.52

[a]Human FLIPR pIC_{50} measured in a Ca^{2+} flux assay. [b]Rat FLIPR measured in a Ca^{2+} flux assay. [c]Stability in rat and human liver microsomes reported as hepatic extraction ratio(s). Primary assays have been run in triplicate with the mean value reported. Standard deviation in all cases was less than two-fold.

Four of the racemic imidazopyridine analogs (**21**, **23**, **25**, **27**) were purified by chiral HPLC and the enantiomers were submitted for testing (**Table 3**). One enantiomer from each racemate was responsible for P2X7 affinity (**1**, **28-30**) with the other enantiomer possessing human and rat P2X7 IC_{50}s > 1000 nM (data not shown). Importantly, the rat affinity for the active enantiomers was improved over the racemates with rP2X7 IC_{50}s now in the 100 to 300 nM range. Mouse P2X7 IC_{50}s and human P2X7 K_is were generated for **1**, **28-30** and were found to be in good agreement with human Ca^{2+} mobilization data. The active enantiomer of **27**, **1** (JNJ 54166060), possessed single digit potency in both human functional and binding assays with an hP2X7 IC_{50} = 4 nM and hP2X7 K_i = 7 nM.

Table 3. Human, rat, and mouse P2X7 data for compounds **1**, **28-30**.

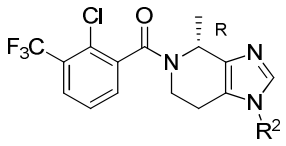

Compd	R^2	hP2X7 IC_{50} (nM)[a]	rP2X7 IC_{50} (nM)[b]	mP2X7 IC_{50} (nM)[c]	hP2X7 K_i (nM)[d]
28	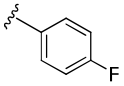	67	303	45	40

29	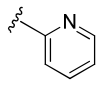	15	116	20	32
1	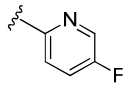	4	115	72	7
30	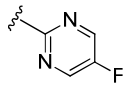	34	300	38	22

[a]Human FLIPR pIC_{50} measured in a Ca^{2+} flux assay. [b]Rat FLIPR measured in a Ca^{2+} flux assay. [c]Mouse FLIPR measured in a Ca^{2+} flus assay. [d]Human K_i measured with [^{3}H]-**5** as the binding ligand. All assay data has been run in triplicate with the mean value reported. Standard deviation in all cases was less than two-fold.

To confirm the structural assignment of our compounds we submitted **1** and its enantiomer (**31**) for absolute stereochemical determination via X-ray crystallography. The single crystal X-ray structures for the two compounds are shown in **Figure 2**. The absolute stereochemistry of the compounds was determined as depicted with the Flack parameter[24] = -0.004 and -0.015 for **1** and **31**, respectively. There were no hydrogen bond interactions or solvates within the crystals with the pyridine and phenyl substituents off the imidazopyrazine core adopting planar geometry. The asymmetric unit contained one disordered molecule of **1** and one fully ordered molecule of **31**.

Figure 2. Single crystal structures and stereo chemical assignment of **1** and **31**.

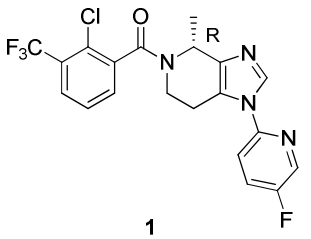

1

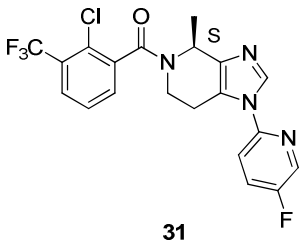

31

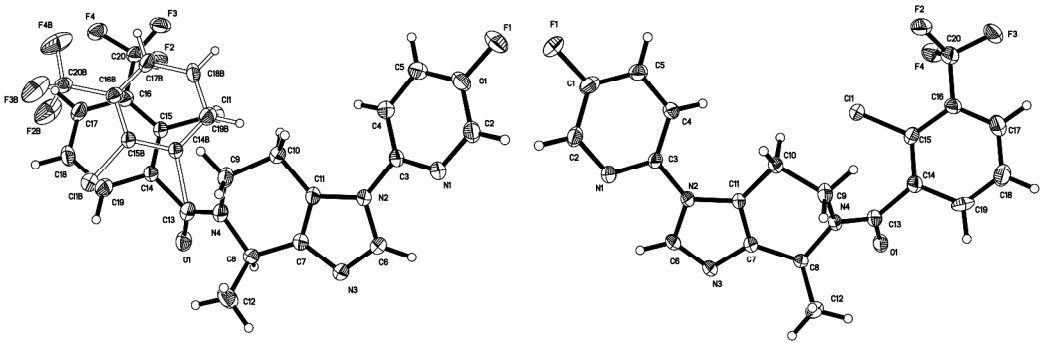

Further in vitro characterization of **1** and **28**-**30** are shown in **Table 4**. The compounds were assessed for liver microsomal stability (HLM/RLM), plasma protein binding (PPB), cytochrome P450 (CYP) inhibition (5 isoforms), solubility (pH2/pH7), and counter screened against the hERG channel. The compounds tested possessed no CYP or hERG liabilities, measurable solubility, and moderate free fraction in both human and rat plasma. Improvements in microsomal stability were observed with 4-F substitution at the R2 substituent with the nitrogen containing heterocycles enhancing solubility across physiologically relevant pH ranges. Indeed a metabolite identification study on **1** in liver microsomes revealed no oxidation on the fluoropyridine substituent with the major metabolite in human being oxidation on the imidazopyridine core. Subsequent isozyme mapping in recombinant human CYPs determined the metabolism of **1** is primarily driven by the CYP3A isoform. There was no evidence of CYP3A time dependent inhibition (TDI) for **1** up to concentrations of 10 μM. In combination with in vitro potency, **1** was identified as a lead candidate for the P2X7 program due to a number of favorable properties including metabolic stability in HLMs, high permeability with no evidence of efflux in Caco-2 cells, moderate free fractions in plasma, no hERG liability, measurable solubility, and P2X7 selectivity as assessed by a CEREP panel and Upstate® kinase panel (Eurofins-CEREP, www.eurofins.com, EMD Millipore, www.emdmillipore.com, no inhibition >50% @ 1 uM). The full in vitro profile of **1** is shown in **Figure 3**.

Table 4. ADME data for compounds **1, 28-30**.

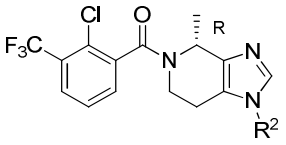

Compd	R^2	HLM/ RLM[a]	h/r PPB[b]	CYPs IC_{50} (μM)[c]	hERG dofet IC_{50} (μM)[d]	Solub. pH2/pH7 (μM)
28	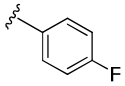	0.36/0.40	96/97.5	> 10	> 10	165/14
29	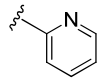	0.63/0.85	95.3/97.4	> 10	> 10	>400/20
1	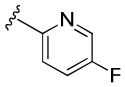	0.35/0.64	94.5/94.9	> 10	> 10	>400/29
30	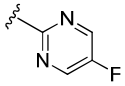	<0.3/0.73	95.2/96.2	2C19 = 7.8	> 10	>400/4

[a]Stability in rat and human liver microsomes reported as hepatic ratio(s). [b]Human and rat plasma protein binding reported as % bound. [c]Screening CYP inhibition data obtained from human liver microsomes. [d]hERG IC_{50} as measured in an [^{3}H]astemizole competition binding assay in HEK-293 cells expressing the hERG channel.

Figure 3. In vitro profile of **1**.

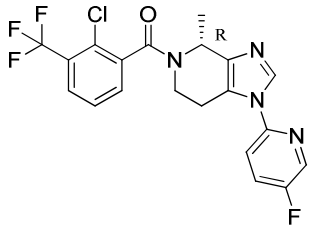

1

h/r/m P2X7 IC_{50} (nM) = 4/115/72
h/r P2X7 K_i (nM) = 7/8
h/m P2X7 Whole Blood IC_{50} (nM) = 92/160
LM h/r/m/d/mk = 0.35/0.67/0.56/0.33/0.41
CYP IC_{50} (μM) all > 10
h/r/m PPB (%) = 94.5/94.9/95.5
rBB = 98.5
hERG IC_{50} (dof. μM) >10
Caco-2 BA/AB = 35/65
solubility pH2/pH7 (μM) = >400/29
Cerep panel = clean @ 1μM
Upstate panel = clean @ 1 μM
CYP phenotyping = CYP3A4
TDI = clean below 10 μM

To gauge the viability of **1** for a CNS indication, central target engagement was assessed via ex vivo P2X7 occupancy in rat brain hippocampal tissue sections using tritiated **5** as the radiotracer.[25] Following oral administration, **1** exhibited dose dependent occupancy in rat brain with an ED_{50} = 2.3 mg/kg corresponding to an EC_{50} = 125 ng/ml and 362 ng/ml in the plasma and brain, respectively. Although the brain concentrations are ~3 fold greater than plasma levels, free plasma and free brain concentrations are similar after correcting for brain binding (1.5% free) and plasma protein binding (5.5% free) with an unbound brain to plasma partition ratio ($K_{p\,u,u}$) of 0.84. Such a $K_{pu,u}$ suggests a limited impact of efflux, in line with Caco-2 in vitro data. Additionally, the free IC_{50}s from this study match in vitro P2X7 potency where the unbound plasma IC_{50} = 6.4 ng/mL (15 nM) and the unbound brain IC_{50} = 5.4 ng/mL (12 nM) (**Figure 4**).

Figure 4. Ex vivo P2X7 occupancy with compound **1** in rat brain; dose dependency following oral administration (n = 3 per dose ± SEM). P2X7 occupancy was measured 30 min after drug administration using tritiated **5** as the radiotracer.

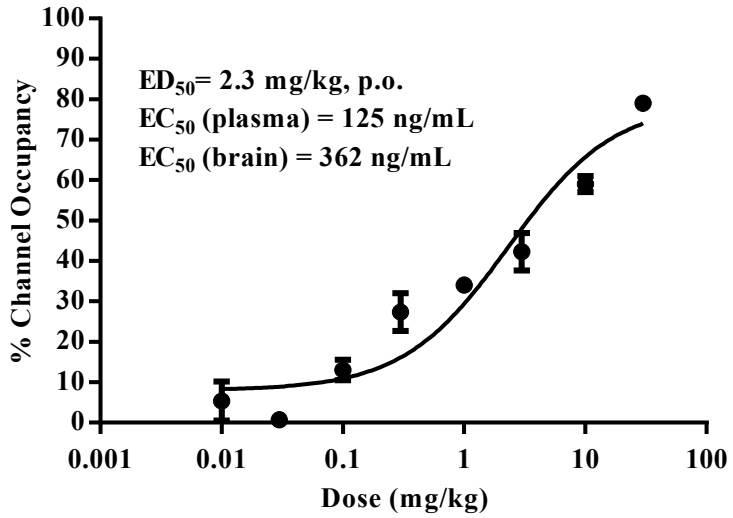

The pharmacokinetic parameters for **1** in rat, dog, and monkey are shown in **Table 5**. Across the three species, there is a strong correlation between predicted and measured clearance values. The predicted in vitro clearance from liver microsomal data for **1** was within 2-fold from the clearance observed in vivo: 35 mL/min/kg vs. 30 mL/min/kg measured for rat; 10 mL/min/kg vs. 5.5 ml/min/kg measured for dog; and 18 ml/min/kg vs. 14 ml/min/kg measured for cynomolgus monkey. High oral bioavailability was observed across three species (%F > 50) with the C_{max} achieved at 1 h from oral administration. Given the high degree of concordance between in vitro and in vivo clearance values across three pre-clinical species, allometric scaling was considered suitable to predict the human dose of **1**. Since the human and rat P2X7 K_i and PPB values were similar (r/h P2X7 K_i = 7 nM, r/h PPB ~ 95%) we used the plasma EC_{50} from the rat dose response experiment of 125 ng/mL as the trough for human plasma concentration. To maintain the plasma concentration above 125 ng/mL a dose of 120 mg QD was predicted for **1** in human with a CL = 2.8 mL/min/kg, Vss = 2.0 L/kg, $t_{1/2}$ = 8.3 hr, and F = 85%.

Table 5. Pharmacokinetic parameters of **1**.

	In vitro from LMs	IV			PO		
	CL[a] (ml/min/kg)	CL[a] (ml/min/kg)	Vss[b] (L/kg)	$t_{1/2}$[c] (hr)	C_{max}[d] (ng/mL)	t_{max}[e] (hr)	F (%)
Rat	36.8	30	3.8	1.7	375	1	55
Dog	10.3	5.5	3.6	11.9	1249	0.5	>100
Monkey	18.2	14	2.1	4.2	389	2.3	54
Human (predicted)	7.3	2.8	2.0	8.3	--	--	85

[a] = Clearance, [b] = Volume of Distribution at steady state [c] = IV half live, [d] = Maximum concentration [e] = Time of maximum concentration

As part of the preclinical toxicology package a single dose and repeat dose toleration study were run in male rats with **1** (**Figure 5**). To meet the compound requirements for the studies additional material was synthesized using **Scheme 2** and the route was found to be scalable. In the repeat dose study, animals were administered **1** at 62.5, 125 or 250 mg/kg/day for 4 days with necropsy performed on day 5. **1** was well tolerated in both the single and repeat dose studies with adequate exposures and no noted CNS side effects. In the single dose experiment increasing exposures were observed up to the 1000 mg/kg dose with a t_{max} of 24 hours for all doses tested. In the repeat dose study no conclusive trends could be extrapolated from the 1 and 4 day exposure data. The histology findings in both studies were considered mild with dose-related increases in total serum cholesterol observed at the 125 and 250 mg/kg/day repeat doses. In addition, one rat dosed at 250 mg/kg/day showed minimal central lobular hepatocellular degeneration and necrosis. Overall, the safety profile observed in the toleration studies supported further development of the molecule.

Figure 5. Single dose and repeat dose toleration studies of **1** in male rats.

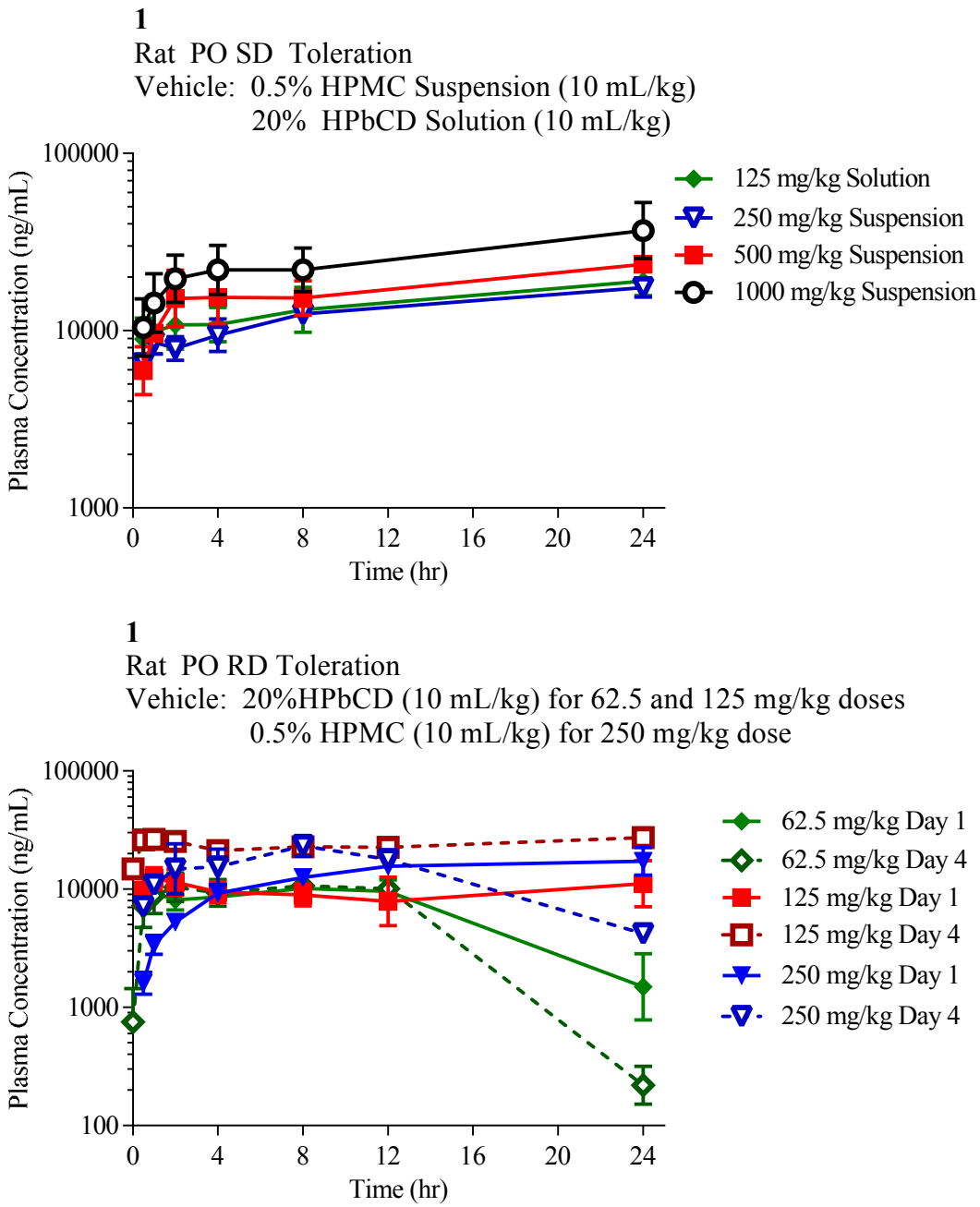

With the preclinical package for **1** nearing completion a discrepancy was identified in a definitive CYP inhibition study. In this study, **1** was found to be a potent inhibitor of CYP3A

with an IC_{50} = 2 μM. This data was at odds with the original screening CYP inhibition data, where **1** showed no significant CYP3A inhibition up to a concentration of 10 μM. Further investigation of the screening CYP inhibition assay revealed that 1-OH-midazolam and 4-OH-midazolam, the two metabolites mediated by CYP3A, co-eluted in the LC-MS assay.[26] When these metabolites were chromatographically resolved, **1** was found to only inhibit the formation of 1-OH-midazolam (IC_{50} = 2.2 μM) and not 4-OH-midazolam (IC_{50} > 10 μM) (**Table 6**). Thus the lack of inhibition of 4-OH-midazolam masked **1**'s CYP3A inhibition when these metabolites co-eluted in the screening assay. The CYP3A enzyme contains a large active site that bears multiple binding orientations, such that the use of multiple CYP3A probes (e.g. midazolam, nifedipine, and testosterone) are required to adequately assess the inhibitory potential of drugs. However, to our knowledge this is the first report of the regioselective inhibition of midazolam by a potential drug candidate.[27] In contrast, ketoconazole, a widely recognized CYP3A inhibitor, exhibited similar inhibition potency at 1-OH midazolam and 4-OH midazolam with IC_{50} values of 9.1 and 7.4 nM, respectively. Overall, given the drug-drug interaction risk, both as perpetrator and as victim, with progressing a potent CYP3A inhibitor whose primary route of clearance is CYP3A mediated; development of **1** was stopped in favor of alternative compounds.

Table 6. Percent inhibition of 1-OH and 4-OH midazolam fromation, **1** vs. Ketoconazole

1			**Ketoconazole (CYP3A4 positive control)**		
Concentration (μM)	1-OH-Midazolam % inhibition	4-OH-Midazolam % inhibition	Concentration (μM)	1-OH-Midazolam % inhibition	4-OH-Midazolam % inhibition
0.313	20	0.1	0.005	34	37
0.625	29	-5	0.01	53	57
1.25	41	-10	0.02	70	74
2.5	52	-13	0.04	82	85
5	63	-13	0.08	90	92
10	74	-4	0.16	94	95

Conclusion

In summary, we have demonstrated that this series of novel 4,5,6,7-tetrahydro-imidazo[4,5-c]pyridines are potent and selective P2X7 antagonists. Optimization of the imidazopyridine core led to compounds with improved liver microsomal stability and P2X7 rat affinity. Compound **1** (JNJ 54166060) was identified as a lead candidate for the P2X7 program with an excellent in vitro profile. In conjunction with ex vivo autoradiography and pharmacokinetic parameters across three pre-clinical species, we were able to predict the human PK profile for **1** and this analysis suggested that **1** would have a human PK profile suitable to treat depressive disorders (i.e. 24 h coverage, oral administration, brain penetration). Preclinical toxicology established that **1** was well tolerated in rats with no behavioral side effects and no major histopathology findings related to drug treatment. Finally, **1** was found to possess a unique CYP profile and was determined to be a regioselective inhibitor of CYP3A; inhibiting the formation of 1-OH midazolam but not 4-OH midazolam.

Experimental Section

In obtaining the compounds described the following experimental and analytical protocols were followed unless otherwise indicated. Anhydrous solvents were obtained from a GlassContour solvent dispensing system. Reagents were purchased from commercial suppliers and were used without purification. The reaction mixtures were magnetically stirred at room temperature (rt) under a nitrogen atmosphere. Where solutions were "dried," they were generally dried over a drying agent such as Na_2SO_4 or $MgSO_4$. Where mixtures, solutions, and extracts were "concentrated", they were typically concentrated on a rotary evaporator under reduced pressure. Reactions under microwave irradiation conditions were carried out in a Biotage Initiator or CEM

Discover instrument. Normal-phase silica gel column chromatography (sgc) was performed on silica gel (SiO_2) using prepackaged cartridges, eluting with 2 M NH_3/MeOH in CH_2Cl_2 or EtOAc in hexanes unless otherwise indicated. Nuclear magnetic resonance (NMR) spectra were obtained on Bruker model DRX spectrometers. The format of the ^1H NMR data below is: chemical shift in ppm downfield of the tetramethylsilane reference (multiplicity, coupling constant J in Hz, integration). High resolution mass spectrometry data were obtained with a Bruker μTOf detector in positive mode, a Zorbax SB-C18 3.5 μM, 2.1 x 50 mm column at 40 °C, an acetonitrile/water with 0.05% formic acid gradient over 7 min, and a flow rate of 0.3 mL/min. Calculated (calcd.) mass corresponds to the exact mass. Chemical names were generated using ChemDraw Ultra 6.0.2 (CambridgeSoft Corp., Cambridge, MA) or ACD/Name Version 9 (Advanced Chemistry Development, Toronto, Ontario, Canada). All compounds tested were of a minimum of 98% purity as determined by HPLC. The HPLC methods used for purity determinations are as follows: Analytical LCMS was obtained on an Agilent 1100/1200 series LCMS with ESI in positive mode and a scan range of 100-700 amu. Samples were run on an Halo C18 column (2.7um, 50 x 3 mm), with a mobile phase of 5-99% ACN in 0.05% TFA over 3.5 min and then held at 99% ACN for 0.5 min, at a flow rate of 1 mL/min (Temperature = 50 °C). Analytical MS was obtained in flow injection mode on an Agilent 1100/1200 Series ESI-SQD in positive mode with a scan range of 100-1000 amu using a mobile phase of 75% ACN: 24.9% H2O: 0.1% TFA at a flow rate of 0.4 mL/min (Temperature = 50 °C). Chiral compounds were analyzed by chiral HPLC or chiral SFC and demonstrated to have ≥ 98% ee.

Representative Procedure A. Step 1. 1-(pyridin-2-yl)-1H-imidazo[4,5-c]pyridine (7a). A solution of 5-azabenzimidazole (1.00 g, 8.40 mmol), 2-bromopyridine (1.30 g, 8.40 mmol), copper (I) oxide (0.13 g, 0.84 mmol), 8-hydroxyquinoline (0.24 g, 1.68 mmol), and

Cs_2CO_3 (5.50 g, 16.8 mmol) in DMSO (4 mL) was irradiated in a microwave apparatus for 1 hour at 140 °C. The reaction was diluted with H_2O (100 mL) and extracted with EtOAc (75 mL x 3). The organic layers were combined, dried (Na_2SO_4), and concentrated. Chromatography of the resulting residue (SiO_2; MeOH (NH_3):DCM) gave the title compound (0.45 g, 25%). ^{1}H NMR (600 MHz, DMSO) δ 9.18 – 9.04 (m, 2H), 8.71 – 8.63 (ddd, J = 4.7, 2.0, 0.9 Hz, 1H), 8.54 – 8.44 (d, J = 5.6 Hz, 1H), 8.32 – 8.23 (dd, J = 5.6, 1.0 Hz, 1H), 8.20 – 8.07 (ddd, J = 8.3, 7.4, 1.9 Hz, 1H), 8.05 – 7.97 (dt, J = 8.2, 1.0 Hz, 1H), 7.56 – 7.43 (ddd, J = 7.4, 4.9, 0.9 Hz, 1H). MS (ESI): mass calculated for $C_{11}H_8N_4$, 196.07; m/z found 197.1 $[M+H]^+$.

Step 2. 5-Benzyl-1-(pyridin-2-yl)-4,5,6,7-tetrahydro-1H-imidazo[4,5-c]pyridine (8). To a solution of **7a** (0.20 g, 1.02 mmol) in DCM (25 mL) was added benzyl bromide (0.12 g, 1.02 mmol). The reaction was let stir for 4 h then concentrated. The resulting solid was dissolved in MeOH (10 mL) and $NaBH_4$ (0.05 g, 1.4 mmol) was added slowly. After 5 h, the reaction was quenched with a small amount of water and concentrated. Chromatography of the resulting residue (SiO_2; MeOH (NH_3):DCM) gave the title compound (0.20 g, 68%). ^{1}H NMR (500 MHz, $CDCl_3$) δ 8.76 – 8.66 (m, 1H), 8.55 – 8.39 (m, 2H), 8.14 – 8.03 (m, 1H), 7.32 (ddt, J = 22.0, 11.6, 7.5 Hz, 6H), 3.89 (s, 1H), 3.78 (d, J = 5.4 Hz, 2H), 3.63 (s, 1H), 2.99 (t, J = 5.5 Hz, 1H), 2.83 (tt, J = 26.6, 5.6 Hz, 3H). MS (ESI): mass calculated for $C_{18}H_{18}N_4$, 290.2; m/z found 291.2 $[M+H]^+$.

Step 3. 1-(Pyridin-2-yl)-4,5,6,7-tetrahydro-1H-imidazo[4,5-c]pyridine (9). To a solution of 5-benzyl-1-(pyridin-2-yl)-4,5,6,7-tetrahydro-1H-imidazo[4,5-c]pyridine (0.13 g, 0.45 mmol) in DCE (5 mL) was added 1-chloroethyl chloroformate (0.10 mL , 0.90 mmoL). The reaction was let stir for 15 min then heated at reflux for 4 h. The reaction was let cool, concentrated, dissolved in MeOH and heated again at 60 °C for 1 h. The reaction was

concentrated and the product was used in the next step without further purification (0.075 g, 83%). ^{1}H NMR (400 MHz, DMSO): δ 9.17 (s, 2H), 9.04 (d, J = 4.9 Hz, 1H), 7.72 -7.28 (m, 2H), 4.46 (t, J = 1.3 Hz, 2H), 3.49 (t, J = 6.0 Hz, 2H), 3.38 (s, 2H). MS (ESI): mass calculated for $C_{11}H_{12}N_4$, 200.1; m/z found 201.2 $[M+H]^+$.

Step 4. (2-Chloro-3-(trifluoromethyl)phenyl)(1-(pyridin-2-yl)-6,7-dihydro-1H-imidazo[4,5-c]pyridin-5(4H)-yl)methanone (12). A solution of 1-(pyridin-2-yl)-4,5,6,7-tetrahydro-1H-imidazo[4,5-c]pyridine (**9**) (0.050 g, 0.25 mmol), 2-chloro-3-trifluoromethyl benzoic acid (0.056 g, 0.25 mmol), HATU (0.10 g, 0.26 mmol, and DIPEA (0.09 mL, 0.50 mmol) in DMF (2 mL) was stirred for 30 min. The reaction was diluted with EtOAc (15 mL) and washed with H_2O (3 x 10 mL). The organic layers were combined, dried (Na_2SO_4), and concentrated. Chromatography of the resulting residue (SiO_2; MeOH (NH_3):DCM) gave the title compound (22 mg, 22%). ^{1}H NMR (400 MHz, $CDCl_3$) δ 8.52 (dd, J = 4.9, 1.8 Hz, 1H), 8.02 (d, J = 18.1 Hz, 1H), 7.92 – 7.71 (m, 2H), 7.58 – 7.40 (m, 2H), 7.37 – 7.28 (m, 2H), 5.12 – 4.78 (m, 1H), 4.51 – 4.19 (m, 2H), 3.97 (ddd, J = 13.4, 12.7, 9.9 Hz, 1H), 3.61 – 3.45 (m, 1H), 3.27 – 2.82 (m, 2H). HRMS calc. for $C_{19}H_{14}ClF_3N_4O$ $[M+H]^+$ 407.0881, found 407.0869.

Representative Procedure B. Step 1. 2-Chloro-3-(trifluoromethyl)benzoyl chloride (18). To a suspension of 2-chloro-3-(trifluoromethyl)benzoic acid (15 g, 67 mmol) and catalytic DMF (0.06 mL, 0.67 mmol) in DCM (150 mL) was added oxalyl chloride (6.8 mL, 80 mmol) dropwise. The reaction was let stir (vigorous bubbling) for 4 h and concentrated to an oily solid which became solid after overnight drying on high vacuum.

Step 2. (2-chloro-3-(trifluoromethyl)phenyl)(1-(5-fluoropyridin-2-yl)-4-methyl-1H-imidazo[4,5-c]pyridin-5(4H)-yl)methanone (19). To a solution of **7a** (0.70 g, 3.27 mmol) in

THF (20 mL) was added **18** (0.87 g, 3.60 mmol) dropwise. The reaction was let stir for 1 h then cooled to – 78 °C. To the cooled solution was added 3M MeMgBr in Et_2O (1.31 mL, 3.92 mmoL) and the reaction was let come to room temperature. The mixture was then quenched with 1N NaOH (50 mL) and extracted with EtOAc (3 x 30 mL). The organic layers were combined, dried (Na_2SO_4), and concentrated. Chromatography of the resulting residue (SiO_2; MeOH (NH_3):DCM) gave the title compound (770 mg, 54%). ^{1}H NMR (400 MHz, $CDCl_3$) δ 8.43 – 8.34 (m, 1H), 7.92 – 7.73 (m, 2H), 7.70 – 7.33 (m, 4H), 6.08 (dtd, J = 19.7, 11.7, 8.0 Hz, 3H), 1.54 (t, J = 7.0 Hz, 3H). MS (ESI): mass calculated for $C_{20}H_{13}ClF_4N_4O$, 436.07; m/z found 437.1 $[M+H]^+$.

Step 3. (2-chloro-3-(trifluoromethyl)phenyl)(1-(5-fluoropyridin-2-yl)-4-methyl-6,7-dihydro-1H-imidazo[4,5-c]pyridin-5(4H)-yl)methanone (27). To a solution of **19** (0.80 g, 1.83 mmol) in degassed EtOH (25 mL) was added palladium on carbon (0.20 mg, 0.19 mmol). The reaction was placed under an atmosphere of hydrogen and let stir for 48 h. The reaction was diluted with DCM and filtered through a pad of Celite ©. The solvent was concentrated and chromatography of the resulting residue (SiO_2; MeOH (NH_3):DCM) gave the title compound (500 mg, 62%). 1H NMR (500 MHz, CDCl3) δ 8.45 – 8.30 (m, 1H), 7.94 (dd, J = 18.2, 10.7 Hz, 1H), 7.76 (d, J = 5.7 Hz, 1H), 7.67 – 7.43 (m, 3H), 7.43 – 7.30 (m, 1H), 5.81 (dd, J = 13.3, 6.7 Hz, 1H), 5.07 (d, J = 5.6 Hz, 1H), 4.52 (d, J = 6.7 Hz, 1H), 3.61 – 3.31 (m, 1H), 3.08 – 2.69 (m, 1H), 1.63 - 145 (m, 3H). HRMS calc. for $C_{20}H_{13}ClF_4N_4O$ $[M+H]^+$ 439.0943, found 439.0957.

Step 4. (*R*)-(2-chloro-3 (trifluoromethyl)phenyl)(1-(5-fluoropyridin-2-yl)-4-methyl-6,7-dihydro-1H-imidazo[4,5-c]pyridin-5(4H)-yl)methanone (1). The title compound was obtained as a single enantiomer by Chiral SFC purification performed using CHIRALCEL OD-H (5 μm, 250x20 mm) and a mobile phase of 72% CO_2, 28% 1:1 EtOH:iPrOH. The enantiomeric

purity was confirmed by analytical SFC using Whelk-al (S,S) (250x4.6 mm) and a mobile phase of 60% CO_2, 40% MeOH over 7 minutes (100% single enantiomer, 4.03 min retention time) (0.16 g, 41%). ^{1}H NMR (500 MHz, $CDCl_3$) δ 8.43 – 8.32 (m, 1H), 7.94 (dd, J = 18.3, 11.2 Hz, 1H), 7.80 – 7.70 (m, 1H), 7.65 – 7.29 (m, 4H), 5.91 – 5.74 (m, 1H), 5.14 – 4.46 (m, 1H), 3.60 – 3.30 (m, 1H), 3.30 – 3.04 (m, 1H), 3.06 – 2.68 (m, 1H), 1.76 – 1.35 (m, 3H). ^{13}C NMR (126 MHz, $CDCl_3$) δ 165.95 – 165.79 (s), 139.33 – 139.10 (d, J = 8.8 Hz), 137.50 – 137.15 (m), 135.54 – 135.31 (m), 131.24 – 131.08 (s), 130.68 – 130.52 (s), 130.42 – 130.26 (s), 128.08 – 127.83 (t, J = 5.7 Hz), 127.50 – 127.13 (m), 126.23 – 125.85 (dd, J = 20.4, 7.6 Hz), 123.69 – 123.54 (s), 122.56 – 122.40 (s), 116.00 – 115.72 (m), 52.32 – 52.16 (s), 47.41 – 47.25 (s), 41.25 – 41.09 (s), 35.57 – 35.41 (s), 24.49 – 24.19 (m), 19.96 – 18.59 (m). HRMS calc. for $C_{20}H_{13}ClF_4N_4O$ $[M+H]^+$ 439.0943, found 439.0957. Specific rotation: $[\alpha]^{20}_D$ – 52.6 (c 0.5, $CHCl_3$).

The following intermediates were prepared in a manner analogous to Representative Procedure A. Step 1.

1-Phenyl-1H-imidazo[4,5-c]pyridine. (40%). MS (ESI): mass calculated for $C_{12}H_9N_3$, 195.08; m/z found 196.1 $[M+H]^+$.

1-(Pyrazin-2-yl)-1H-imidazo[4,5-c]pyridine. (24%). MS (ESI): mass calculated for $C_{10}H_7N_5$, 197.07; m/z found 198.1 $[M+H]^+$.

1-(5-Fluoropyridin-2-yl)-1H-imidazo[4,5-c]pyridine. (37%). MS (ESI): mass calculated for $C_{11}H_7FN_4$, 214.07; m/z found 215.1 $[M+H]^+$.

1-(4-fluorophenyl)-1H-imidazo[4,5-c]pyridine. (34%) MS (ESI): mass calculated for $C_{12}H_8FN_3$, 213.07; m/z found 214.1 $[M+H]^+$.

1-(pyrimidin-2-yl)-1H-imidazo[4,5-c]pyridine. (24%) MS (ESI): mass calculated for $C_{10}H_7N_5$, 197.07; m/z found 198.1 $[M+H]^+$.

1-(5-fluoropyrimidin-2-yl)-1H-imidazo[4,5-c]pyridine. (17%) MS (ESI): mass calculated for $C_{10}H_6FN_5$, 215.06; m/z found 216.1 $[M+H]^+$.

1-(3-fluoropyridin-2-yl)-1H-imidazo[4,5-c]pyridine. (20%) MS (ESI): mass calculated for $C_{11}H_7FN_4$, 214.07; m/z found 215.1 $[M+H]^+$.

The following intermediates were prepared in a manner analogous to Representative Procedure A. Step 2.

5-Benzyl-1-phenyl-4,5,6,7-tetrahydro-1H-imidazo[4,5-c]pyridine. (89%). MS (ESI): mass calculated for $C_{19}H_{19}N_3$, 289.16; m/z found 290.0 $[M+H]^+$.

5-Benzyl-1-(pyrazin-2-yl)-4,5,6,7-tetrahydro-1H-imidazo[4,5-c]pyridine. (69%). MS (ESI): mass calculated for $C_{17}H_{17}N_5$, 291.15; m/z found 292.0 $[M+H]^+$.

5-Benzyl-1-(5-fluoropyridin-2-yl)-4,5,6,7-tetrahydro-1H-imidazo[4,5-c]pyridine. (87%). MS (ESI): mass calculated for $C_{18}H_{17}FN_4$, 308.14; m/z found 309.2 $[M+H]^+$.

The following intermediates were prepared in a manner analogous to Representative Procedure A. Step 3.

1-Phenyl-4,5,6,7-tetrahydro-1H-imidazo[4,5-c]pyridine. (79%). MS (ESI): mass calculated for $C_{12}H_{13}N_3$, 199.11; m/z found 200.1 $[M+H]^+$.

1-(Pyrazin-2-yl)-4,5,6,7-tetrahydro-1H-imidazo[4,5-c]pyridine. (75%). MS (ESI): mass calculated for $C_{10}H_{11}N_5$, 201.10; m/z found 202.1 $[M+H]^+$.

1-(5-Fluoropyridin-2-yl)-4,5,6,7-tetrahydro-1H-imidazo[4,5-c]pyridine. (78%). MS (ESI): mass calculated for $C_{11}H_{11}FN_4$, 218.10; m/z found 219.1 $[M+H]^+$.

The following compounds were prepared in a manner analogous to Representative Procedure A. Step 4.

(2,3-Dichlorophenyl)(1-phenyl-6,7-dihydro-1H-imidazo[4,5-c]pyridin-5(4H)-yl)methanone (10). (75%). ^{1}H NMR (400 MHz, $CDCl_3$) δ 7.67 (s, 0.4H), 7.60 (s, 0.6H), 7.56 – 7.39 (m, 4H), 7.33 – 7.20 (m, 5H), 4.96 – 4.90 (m, 1H) , 4.46 – 4.20 (m, 2H), 4.03 – 3.92 (m, 1H), 3.60 – 3.43 (m, 1H), 2.67 (ddd, J = 20.9, 15.5, 6.8 Hz, 1H). HRMS calc. for $C_{19}H_{15}Cl_2N_3O$ $[M+H]^+$ 372.0665, found 372.0682.

(2-Chloro-3-(trifluoromethyl)phenyl)(1-phenyl-6,7-dihydro-1H-imidazo[4,5-c]pyridin-5(4H)-yl)methanone (11). (90%). ^{1}H NMR (400 MHz, $CDCl_3$) δ 7.79 – 7.74 (m, 1H), 7.68 (s, 0.4H), 7.60 (s, 0.6H), 7.56 – 7.39 (m, 5H), 7.34 – 7.28 (m, 2H), 4.99 – 4.90 (m, 1H) , 4.45 – 4.27 (m, 2H), 3.93 (ddd, J = 12.8, 7.2, 5.2 Hz, 1H), 3.60 – 3.45 (m, 1H). HRMS calc. for $C_{20}H_{15}ClF_3N_3O$ $[M+H]^+$ 406.0929, found 406.0933.

(2-Chloro-3-(trifluoromethyl)pheny1)(1-(pyrazin-2-yl)-6,7-dihydro-lH-imidazo[4,5-c]pyridin-5(4H)-yl) methanone (13). (47%) ^{1}H NMR (400 MHz, $CDCl_3$) δ 8.81 – 8.75 (m, 1H), 8.64 – 8.42 (m, 2H), 8.16 – 8.02 (m, 1H), 7.83 – 7.71 (td, J = 7.5, 1.9 Hz, 1H), 7.60 – 7.40 (m, 2H), 5.08 – 4.80 (m, 1H), 4.50 – 4.23 (m, 2H), 4.10 – 3.94 (ddd, J = 13.0, 6.6, 5.6 Hz, 1H), 3.67 – 3.46 (m, 1H), 3.21 – 2.91 (m, 2H), 2.11 – 1.76 (m, 2H). HRMS calc. for $C_{18}H_{13}ClF_3N_5O$ $[M+H]^+$ 408.0833, found 408.0819.

(2-Chloro-3-(trifluoromethyl)phenyl)(1-(5-fluoropyridin-2-yl)-6,7-dihydro-lH-imidazo[4,5-c]pyridin-5(4H)-yl)methanone (14). (45%) ^{1}H NMR (400 MHz, DMSO) δ 8.59 –

8.51 (m, 1H), 8.28 – 8.17 (m, 1H), 8.04 – 7.92 (m, 2H), 7.84 – 7.63 (m, 3H), 4.91 – 4.54 (dd, J = 92.1, 16.0 Hz, 2H), 4.23 – 4.14 (d, J = 3.0 Hz, 1H), 3.51 – 3.36 (q, J = 5.9, 5.4 Hz, 2H), 3.08 – 2.79 (m, 2H). $[M+H]^+$. HRMS calc. for $C_{19}H_{13}ClF_4N_4O$ $[M+H]^+$ 425.0787, found 425.0781.

(1-(5-Fluoropyridin-2-yl)-4,5,6,7-tetrahydro-1H-benzo[d]imidazol-5-yl)(2-methyl-3-(trifluoromethyl)phenyl)methanone (15). (51%) ^{1}H NMR (400 MHz, DMSO) δ 8.59 – 8.50 (m, 1H), 8.28 – 8.16 (m, 1H), 8.06 – 7.94 (m, 1H), 7.85 – 7.74 (dt, J = 9.1, 4.7 Hz, 2H), 7.63 – 7.46 (m, 2H), 4.95 – 4.48 (m, 1H), 4.22 – 4.06 (m, 1H), 3.49 – 3.37 (q, J = 4.8, 4.3 Hz, 2H), 2.43 – 2.20 (m, 3H). HRMS calc. for $C_{20}H_{16}F_4N_4O$ $[M+H]^+$ 405.1333, found 405.1332.

(2,4-Dichlorophenyl)(1-(5-fluoropyridin-2-yl)-6,7-dihydro-1H-imidazo[4,5-c]pyridin-5(4H)-yl)methanone (16). (74%) ^{1}H NMR (400 MHz, DMSO) δ 8.59 – 8.49 (m, 1H), 8.29 – 8.14 (m, 1H), 8.05 – 7.95 (ddd, J = 6.8, 3.9, 2.2 Hz, 1H), 7.81 – 7.73 (m, 2H), 7.59 – 7.40 (m, 2H), 4.85 – 4.51 (d, J = 16.0 Hz, 1H), 4.37 – 4.08 (m, 1H), 4.08 – 3.87 (m, 1H), 3.60 – 3.41 (m, 1H), 3.07 – 2.83 (m, 2H). HRMS calc. for $C_{18}H_{13}Cl_2FN_4O$ $[M+H]^+$ 391.0523, found 391.0533.

(2-Fluoro-3-(trifluoromethy l)pheny1)(1-(5-fluoropyri- din-2-yl)-6,7-dihydro- lH-imidazo[4,5-c]pyridin-5 (4H)-yl)methanone (17). (96%) ^{1}H NMR (400 MHz, DMSO) δ 8.62 – 8.51 (m, 1H), 8.29 – 8.16 (m, 1H), 8.05 – 7.72 (m, 4H), 7.62 – 7.48 (m, 1H), 4.78 – 4.60 (s, 1H), 4.36 – 4.23 (s, 1H), 4.06 – 3.97 (t, J = 5.7 Hz, 1H), 3.61 – 3.48 (t, J = 5.6 Hz, 1H), 2.96 (m, 2H). HRMS calc. for $C_{19}H_{13}F_5N_4O$ $[M+H]^+$ 409.1082, found 409.1095.

The following intermediates were prepared in a manner analogous to Representative Procedure B. Step 3.

(2-chloro-3-(trifluoromethyl)phenyl)(4-methyl-1-phenyl-1H-imidazo[4,5-c]pyridin-5(4H)-yl)methanone. (52%) MS (ESI): mass calculated for $C_{21}H_{15}ClF_3N_3O$, 417.09; m/z found 418.1 $[M+H]^+$.

(2-chloro-3-(trifluoromethyl)phenyl)(1-(4-fluorophenyl)-4-methyl-1H-imidazo[4,5-c]pyridin-5(4H)-yl)methanone. (49%) MS (ESI): mass calculated for $C_{21}H_{14}ClF_4N_3O$, 435.08; m/z found 436.1 $[M+H]^+$.

(2-chloro-3-(trifluoromethyl)phenyl)(4-methyl-1-(pyrimidin-2-yl)-1H-imidazo[4,5-c]pyridin-5(4H)-yl)methanone. (35%) MS (ESI): mass calculated for $C_{19}H_{13}ClF_3N_5O$, 419.08; m/z found 420.1 $[M+H]^+$.

(2-chloro-3-(trifluoromethyl)phenyl)(1-(5-fluoropyrimidin-2-yl)-4-methyl-1H-imidazo[4,5-c]pyridin-5(4H)-yl)methanone. (37%) MS (ESI): mass calculated for $C_{19}H_{12}ClF_4N_5O$, 437.07; m/z found 438.1 $[M+H]^+$.

(2-chloro-3-(trifluoromethyl)phenyl)(4-methyl-1-(pyrazin-2-yl)-1H-imidazo[4,5-c]pyridin-5(4H)-yl)methanone. (35%) MS (ESI): mass calculated for $C_{19}H_{13}ClF_3N_5O$, 419.08; m/z found 420.1 $[M+H]^+$.

(2-chloro-3-(trifluoromethyl)phenyl)(4-methyl-1-(pyridin-2-yl)-1H-imidazo[4,5-c]pyridin-5(4H)-yl)methanone. (33%) MS (ESI): mass calculated for $C_{20}H_{14}ClF_3N_4O$, 418.08; m/z found 419.1 $[M+H]^+$.

(2-chloro-3-(trifluoromethyl)phenyl)(1-(3-fluoropyridin-2-yl)-4-methyl-1H-imidazo[4,5-c]pyridin-5(4H)-yl)methanone. (38%) MS (ESI): mass calculated for $C_{20}H_{13}ClF_4N_4O$, 436.07; m/z found 437.1 $[M+H]^+$.

The following compounds were prepared in a manner analogous to Representative Procedure B. Step 3.

(2-Chloro-3-(trifluoromethyl)phenyl)(4-methyl-1-phenyl-6,7-dihydro-1H-imidazo[4,5-c]pyridin-5(4H)-yl)methanone (20). (66%) ^{1}H NMR (500 MHz, $CDCl_3$) δ 7.76 (dd, J = 5.1, 2.0 Hz, 1H), 7.65 (d, J = 15.1 Hz, 1H), 7.59 – 7.39 (m, 5H), 7.35 – 7.28 (m, 2H), 5.83 (dd, J = 13.5, 6.7 Hz, 1H), 5.07 (dd, J = 12.3, 10.6 Hz, 1H), 4.19 – 3.99 (m, 1H), 3.61 – 2.93 (m, 1H), 2.75 – 2.35 (m, 1H), 1.99 – 1.90 (m , 3H). HRMS calc. for $C_{21}H_{17}ClF_3N_3O$ $[M+H]^+$ 420.1085, found 420.1072.

(2-Chloro-3-(trifluoromethyl)phenyl)(1-(4-fluorophenyl)-4-methyl-6,7-dihydro-1H-imidazo[4,5-c]pyridin-5(4H)-yl)methanone (21). (40%) ^{1}H NMR (500 MHz, $CDCl_3$) δ 7.79 – 7.73 (m, 1H), 7.62 (d, J = 1.3 Hz, 1H), 7.58 – 7.35 (m, 2H), 7.33 – 7.25 (m, 2H), 7.25 – 7.15 (m, 2H), 5.94 – 5.47 (m, 1H), 5.07 – 4.59 (m, 1H), 4.10 – 3.73 (m, 1H), 3.59 – 2.81 (m, 1H), 2.74 – 2.23 (m, 1H), 1.69 – 1.50 (m, 3H). HRMS calc. for $C_{21}H_{16}ClF_4N_3O$ $[M+H]^+$ 438.0991, found 438.0973.

(2-Chloro-3-(trifluoromethyl)phenyl)(4-methyl-1-(pyrimidin-2-yl)-6,7-dihydro-1H-imidazo[4,5-c]pyridin-5(4H)-yl)methanone (22). (58%) ^{1}H NMR (500 MHz, $CDCl_3$) δ 8.75 – 8.49 (m, 3H), 7.76 (dt, J = 9.6, 4.8 Hz, 1H), 7.59 – 7.42 (m, 2H), 7.21 (ddd, J = 17.7, 8.0, 4.8 Hz, 1H), 5.91 – 5.67 (m, 1H), 5.16 – 4.55 (m, 1H), 3.60 – 2.87 (m, 4H), 1.72 – 1.56 (m, 3H). HRMS calc. for $C_{19}H_{15}ClF_3N_5O$ $[M+H]^+$ 422.0990, found 422.0976.

(2-Chloro-3-(trifluoromethyl)phenyl)(1-(5-fluoropyrimidin-2-yl)-4-methyl-6,7-dihydro-1H-imidazo[4,5-c]pyridin-5(4H)-yl)methanone (23). (52%) ^{1}H NMR (500 MHz, $CDCl_3$) δ 8.61 – 8.38 (m, 3H), 7.82 – 7.70 (m, 1H), 7.58 – 7.32 (m, 2H), 5.90 – 5.60 (m, 1H),

5.19 – 4.54 (m, 1H), 3.66 – 2.82 (m, 3H), 1.81 – 1.29 (m, 3H). HRMS calc. for $C_{19}H_{14}ClF_4N_5O$ $[M+H]^+$ 440.0896, found 440.0886.

(2-Chloro-3-(trifluoromethyl)phenyl)(4-methyl-1-phenyl-6,7-dihydro-1H-imidazo[4,5-c]pyridin-5(4H)-yl)methanone (24). (44%) ^{1}H NMR (500 MHz, $CDCl_3$) δ 8.65 – 8.45 (m, 3H), 7.80 – 7.70 (m, 1H), 7.58 – 7.42 (m, 2H), 7.24 – 7.18 (m, 1H), 5.91 – 5.71 (m, 1H), 5.10 – 4.70 (m, 1H), 3.60 – 2.88 (m, 4H), 1.70 – 1.57 (m, 3H). HRMS calc. for $C_{19}H_{15}ClF_3N_5O$ $[M+H]^+$ 422.0990, found 422.0992.

(2-chloro-3-(trifluoromethyl)phenyl)(4-methyl-1-(pyridin-2-yl)-6,7-dihydro-1H-imidazo[4,5-c]pyridin-5(4H)-yl)methanone (25). (40%) ^{1}H NMR (500 MHz, $CDCl_3$) δ 8.58 – 8.44 (m, 1H), 7.99 (dt, J = 10.8, 8.7 Hz, 1H), 7.93 – 7.80 (m, 1H), 7.80 – 7.72 (m, 1H), 7.59 – 7.43 (m, 2H), 7.41 – 7.24 (m, 2H), 5.91 – 5.72 (m, 1H), 5.20 – 4.58 (m, 1H), 3.63 – 3.29 (m, 1H), 3.29 – 2.76 (m, 2H), 1.74 – 1.60 (m, 3H). HRMS calc. for $C_{19}H_{14}ClF_3N_4O$ $[M+H]^+$ 421.1037, found 421.1039.

(2-Chloro-3-(trifluoromethyl)phenyl)(1-(3-fluoropyridin-2-yl)-4-methyl-6,7-dihydro-1H-imidazo[4,5-c]pyridin-5(4H)-yl)methanone (26). (20%) ^{1}H NMR (500 MHz, $CDCl_3$) δ 8.43 – 8.28 (m, 1H), 7.94 (dd, J = 23.2, 20.8 Hz, 1H), 7.81 – 7.61 (m, 2H), 7.59 – 7.29 (m, 3H), 5.82 (dt, J = 12.9, 6.5 Hz, 1H), 5.06 (dd, J = 13.5, 6.7 Hz, 1H), 4.76 – 4.37 (m, 1H), 3.63 – 2.62 (m, 2H), 1.86 – 1.55 (m, 3H). HRMS calc. for $C_{20}H_{14}ClF_4N_4O$ $[M+H]^+$ 439.0943, found 439.0940.

(2-Chloro-3-(trifluoromethyl)phenyl)(1-(5-fluoropyrimidin-2-yl)-4-methyl-6,7-dihydro-1H-imidazo[4,5-c]pyridin-5(4H)-yl)methanone (27). (62%) ^{1}H NMR (500 MHz, $CDCl_3$) δ 8.61 – 8.38 (m, 3H), 7.82 – 7.70 (m, 1H), 7.58 – 7.32 (m, 2H), 5.90 – 5.60 (m, 1H),

5.19 – 4.54 (m, 1H), 3.66 – 2.82 (m, 3H), 1.81 – 1.29 (m, 3H). HRMS calc. for $C_{20}H_{14}ClF_4N_4O$ $[M+H]^+$ 439.0943, found 439.0940.

The following compounds were prepared in a manner analogous to Representative Procedure B. Step 4.

(R)-(2-chloro-3-(trifluoromethyl)phenyl)(1-(4-fluorophenyl)-4-methyl-6,7-dihydro-1H-imidazo[4,5-c]pyridin-5(4H)-yl)methanone (28). (40%) ^{1}H NMR (500 MHz, $CDCl_3$) δ 7.76 (dd, J = 5.1, 3.2 Hz, 1H), 7.62 (s, 1H), 7.58 – 7.36 (m, 2H), 7.33 – 7.24 (m, 2H), 7.24 – 7.14 (m, 2H), 5.89 – 5.78 (m, 1H), 5.07 (dt, J = 12.3, 6.0 Hz, 1H), 4.77 – 4.39 (m, 1H), 3.62 – 2.86 (m, 1H), 2.77 – 2.28 (m, 1H), 1.80 – 1.10 (m, 3H). HRMS calc. for $C_{21}H_{16}ClF_4N_3O$ $[M+H]^+$ 438.0991, found 438.0988.

(R)-(2-chloro-3-(trifluoromethyl)phenyl)(4-methyl-1-(pyridin-2-yl)-6,7-dihydro-1H-imidazo[4,5-c]pyridin-5(4H)-yl)methanone (29). (44%) ^{1}H NMR (600 MHz, $CDCl_3$) δ 8.59 – 8.45 (m, 1H), 8.01 (dd, J = 20.6, 15.5 Hz, 1H), 7.86 (tdd, J = 8.1, 5.7, 3.8 Hz, 1H), 7.76 (dd, J = 6.3, 4.7 Hz, 1H), 7.58 – 7.28 (m, 4H), 5.82 (dd, J = 14.3, 7.4 Hz, 1H), 4.58 (d, J = 6.5 Hz, 1H), 4.03 (dt, J = 12.2, 6.1 Hz, 1H), 3.34 – 2.80 (m, 2H), 1.69 – 1.44 (m, 3H). HRMS calc. for $C_{19}H_{14}ClF_3N_4O$ $[M+H]^+$ 421.1037, found 421.1039.

(R)-(2-chloro-3-(trifluoromethyl)phenyl)(1-(5-fluoropyrimidin-2-yl)-4-methyl-6,7-dihydro-1H-imidazo[4,5-c]pyridin-5(4H)-yl)methanone (30). (42%) ^{1}H NMR (500 MHz, $CDCl_3$) δ 8.61 – 8.38 (m, 3H), 7.82 – 7.70 (m, 1H), 7.58 – 7.32 (m, 2H), 5.90 – 5.60 (m, 1H), 5.19 – 4.54 (m, 1H), 3.66 – 2.82 (m, 3H), 1.81 – 1.29 (m, 3H). HRMS calc. for $C_{19}H_{14}ClF_4N_5O$ $[M+H]^+$ 440.0896, found 440.0901.

P2X7 Antagonism in Human Peripheral Blood Mononuclear Cells (PBMCs) and Mouse

Human Whole Blood. Human blood was collected using a blood donor program. PBMCs were isolated from blood using a Ficoll density gradient technique. Briefly, blood was laid on Ficoll solution and centrifuged at RT for 20 minutes at 2000 rpm. The buffy layer (between red blood cells and plasma) was carefully collected by aspiration, washed with PBS and centrifuged again at 1500 rpm for 15 minutes. The resulting cell pellet was washed and plated on 96 well-plates for experiments. For the Mouse Human Whole Blood experiments, 150 µl of either mouse or human blood was platted on 96 well- plates. Lipopolysaccharide (LPS) (30 ng/ml) was added to each well and incubated for 1hour. Test compounds were then added and incubated for 30 minutes. The P2X7 agonist, 2'(3')- 0-(4-benzoylbenzoyl) adenosine 5' triphosphate (Bz-ATP) was then added at a final concentration of 0.5 mM (PBMC) or 1 mM (blood). Cells were incubated for an additional 1.5 hours. At that point, supernatant was collected and stored for IL-1β assay using manufacturer's protocol for enzyme- linked immunosorbent assay (ELISA). Data was expressed as percent control, where control is defined as the difference in IL-1β release in LPS+Bz-ATP samples and LPS only samples. Data was plotted as response (% control) versus concentration to generate IC_{50} values.

P2X7 Antagonism in Recombinant hP2X7 Cells: Ca^{2+}Flux. 1321Nl cells expressing the recombinant human, rat or mouse P2X7 channel was cultured in HyQ DME/(HyClone/Dulbecco's Modified Eagle Medium) high glucose supplemented with 10% Fetal Bovine Serum (FBS) and appropriate selection marker. Cells were seeded at a density of 25000 cells/well (96-well clear bottom black walled plates) in 100 µl volume/well. On the day of the experiment, cell plates were washed with assay buffer, containing (in mM): 130 NaCl, 2 KCl, 1 $CaCl_2$, 1 MgCl 2, 10 HEPES, 5 glucose; pH 7.40 and 300 mOs. After the wash, cells were loaded with the Calcium-4 dye (Molecular Device) and incubated in the dark for 60 minutes.

Test compounds were prepared at 250x the test concentration in neat DMSO. Intermediate 96-well compound plates were prepared by transferring 1.2 µL of the compound into 300 µL of assay buffer. A further 3x dilution occurred when transferring 50 µL/well of the compound plate to 100 µL/well in the cell plate. Cells were incubated with test compounds and dye for 30 minutes. Calcium dye fluorescence was monitored in FLIPR as the cells were challenged by adding 50 µL/well of BzATP (final concentration is 250 µM BzATP (human and rat) or 600 µM (mouse)). The fluorescence change was measured 180 seconds after adding the agonist. Peak fluorescence was plotted as a function of test concentration to generate an IC_{50} value.

P2X7 Antagonism in Recombinant hP2X7 Cells: Radioligand binding. Human or rat P2X7 1321Nl cells were collected and frozen @-80° C. On the day of the experiment, cell membrane preparations were made according to standard published methods. The total assay volume was 100 µl: 10 µl compound (l0x)+(b) 40 µl tracer (2.5x)+50 µl membrane (2x). The tracer used for the assay was tritiated A-804598. The compound can be prepared as described in the literature (Donnelly-Roberts, D. Neuropharmacology 2008, 56 (1), 223-229). Compounds, tracer and membranes were incubated for 1 hour @ 4° C. The assay was terminated by filtration (GFB filters pre-soaked with 0.3% PEI) and washed with washing buffer (Tris-HCl 50 mM). The IC_{50} generated in the binding assay was corrected for tracer concentration and affinity of the tracer to derive at the affinity (K) of the test compounds.

Caco-2 Permeability. Caco-2 bi-directional permeability assays were conducted at CEREP according to company's protocol. In brief, Caco-2 cells were seeded onto a 96-well Multiscreen plate™ (Millipore) at a cell density of 1 x 10^5 cells/cm^2 and cultured for at least 21 days before permeability studies were conducted. Test compounds were dissolved in DMSO and added to HBSS-HEPES, pH 7.4 culture media at a final concentration of 10 µM (1 % DMSO v/v). The

working solution was applied to cells on the donor side and incubated at 37 ° C with gentle agitation for 60 and 40 min to determine the A→B and B→A permeability, respectively. Samples were extracted from the donor side at time zero and the end-point and from the receiver side at the end-point time only. Samples were then processed for LC/MS/MS analyses to determine the apparent permeability coefficient (P_{app}) of the test compound in the A→ B and B→A direction as well as the percent recovery.[28]

Plasma Protein Binding. Plasma protein binding was determined by equilibrium dialysis using the RED Device (Thermo Scientific, Rockford, IL) consisting of a Teflon base block and RED Device inserts comprising two (sample and buffer) side-by-side chambers separated by a dialysis membrane. Compounds were prepared as 100 μM DMSO stocks and spiked into 1 mL of mouse, rat, and human plasma (Bioreclamations) to make a final concentration of 1 μM. Plasma (300 μL) was dispensed into wells separated by an 8 kDa-permeable cellulose membrane from wells containing 100 mM potassium phosphate, pH 7.4 (500 μL). Each compound was tested in triplicate. The RED devise was sealed and equilibrium was permitted for 6 h in a 37 °C incubator with gentle agitation at 100 RPM. After incubation, plasma samples were prepared by transferring 10 μL from plasma wells to 90 μL of fresh 100 mM potassium phosphate, pH 7.4, and buffer samples were prepared by transferring 90 μL from buffer wells to 10 μL of naïve plasma. In addition, a reference sample without equilibration was prepared in triplicate by mixing 10 μL of plasma containing 1 μM compound with 90 μL buffer in order to determine compound recovery from the assay. Two-volumes of 1:1 acetonitrile:methanol spiked with the internal standard phenytoin (0.2 μg/mL) were added to reference and samples. Precipitation of plasma protein binding was allowed for 15 min before reference and samples were centrifuge clarified. Supernatant (10 μL) was used for LC/MS/MS analyses.

Brain Tissue Binding. Brain tissue binding was assessed by equilibrium dialysis using the RED device similar to the procedure described for plasma protein binding. Rat brain tissue homogenate, prepared in PBS buffer, pH 7.4 (1:10, w/v), was spiked with compound DMSO stock solution to yield a final concentration of 5 μM. The dialysis was carried out in a shaking incubator at 37 °C for 5 h in triplicate. After incubation, 25 μL of homogenate or 50 μL of buffer was extracted with 50 μL of DMSO and 300 μL of acetonitrile and analyzed by LC/MS/MS using the calibration curves across an appropriate concentration range and quality control samples. The apparent unbound fraction ($f_{u,app}$) was derived from the formula:

$$fu, app = \frac{[\mathrm{A}]buffer}{[\mathrm{A}]homogenate}$$

where $[\mathrm{A}]_{homogenate}$ and $[\mathrm{A}]_{buffer}$ are the concentrations measured in the homogenate and buffer, respectively. The unbound fraction in undiluted brain ($f_{u,\ brain}$) was calculated from the formula

$$fu, brain = \frac{fu, app}{\mathrm{D} + fu, app - \mathrm{D} * fu, app}$$

where D is the dilution factor of 10. Subsequently, the percentage compound bound to brain tissue (% BTB) was calculated from the formula

$$\%\ BTB = (1 - fu, brain) * 100\ \%$$

Liver Microsomal Stability. Microsomal stability studies were conducted on a Biomek® FX Robotic Liquid Handling Workstation (Beckman Coulter, Brea, CA), which consists of a 96-channel pipette head, a 12-postion workstation deck, and a plate incubator. Test compounds (1 μM) were spiked in a reaction mix consisting of 100 mM potassium phosphate buffer (pH 7.4), 3 mM $MgCl_2$, and 0.5 mg/mL liver microsomes from mouse, rat, dog, monkey, and human (BD

Gentest). The reaction was brought to 37 °C and initiated by adding NADPH to a final concentration of 1 mM. After mixing on the plate-deck, 50 μL aliquots were excised from the reaction plate at 0, 5, 10, 20, 40, and 60 min and quenched with four volumes of acetonitrile spiked with 500 μg/nL of the internal standard phenytoin. Quenched plates were centrifuged at 5700 rpm for 10 min at 4 °C, and supernatant was diluted 1:3 in water before LC/MS/MS analysis. The compound half-lives were derived from plots of the ln of percent remaining compound over time to determine the intrinsic clearance. The predicted hepatic clearance was derived from the intrinsic clearance value using equations from the well-stirred model where protein binding in plasma and microsomal proteins is assumed to be similar and the blood to plasma concentration ratio is assumed to be one.[29] The hepatic extraction ratio (ER) was calculated by dividing the predicted hepatic clearance by species blood flow (Q), where Q is 90, 55, 31, 44, and 21.7 mL/min/kg for mouse, rat, dog, monkey, and human, respectively.

Solubility in Aqueous Systems. Solubility in 30 mM phosphate buffers (pH 2 and pH 7), simulated gastric (SGF, 0.2% NaCl in 0.1 N HCl, pH 1.2) and intestinal fluids (FasSIF, 0.029 M phosphate buffer, 5 mM sodium taurocholate, and 1.5 mM lecithin, pH 6.8) was investigated. Compound was dissolved in DMSO solutions at a concentration of 10 mM and was used for the solubility experiment. DMSO solutions (20 μL) are dispensed in 96-well plates, and the solvent is removed by evaporation using a Caliper TurboVap 96 set at 30 °C and a flow rate of 40 Fh. Buffers (400 μL) of interest are added to the residual solids, and the resulting mixtures are stirred at room temperature for 3 days using magnetic stir bars. The samples are then filtered using an AcroPrep 1 mL 96 filter plate, and the supernatant is analyzed for compound concentration, against external standards.

Cocktail CYP Inhibition Assay. DMSO stocks were prepared for test compounds (10 mM) and for the assay positive controls: furafylline (CYP1A2 – 8 mM), quercetin (CYP2C8 – 12 mM), sulfaphenazole (CYP2C9 – 2 mM), *N*-3-benzyl-phenobarbital (CYP2C19 – 1.2 mM), quinidine (CYP2D6 – 0.16 mM), and ketoconazole (CYP3A – 0.16 mM). In a solution of 1:1 acetonitrile:water, stocks were diluted 10-fold and serial diluted in 2-fold increments. For test compounds, the final incubation concentrations were 10, 5, 2.5, 1.25, 0.63, and 0.3 μM. To simultaneously measure the activity of multiple CYPs in the same incubation, a cocktail probe solution was prepared that contained six substrates at the following final concentrations: phenacetin (CYP1A2 – 50 μM), paclitaxel (CYP2C8 – 10 μM), diclofenac (CYP2C9 – 4 μM), *S*-mephenytoin (CYP2C19 – 30 μM), dextromethorphan (CYP2D6 – 3 μM), and midazolam (CYP3A – 2 μM). Human liver microsomes (BD Gentest) from a mixed donor pool were prepared in 0.1 mM potassium phosphate buffer (pH 7.4) supplemented with 3 mM $MgCl_2$ and pre-incubated for 5 min at 37 °C. Human liver microsomes (0.1 mg of protein/mL) were then mixed with the cocktail probe solution, test compounds or assay positive controls, and the reaction was initiated by the addition of NADPH (1 mM final concentration). The catalysis of probe substrates was permitted for 15 min at 37 °C and quenched in one volume of 1:1 acetonitrile:methanol mixture containing the internal standard phenytoin (0.2 μg/mL). Samples were vortexed for 2 min and centrifuged for 10 min. Supernatant (300 μL) was diluted in water (125 μL), mixed, and used for LCMS/MS analysis. A 20-μL aliquot was analyzed for probe metabolite formation using a Shimadzu LC-20A HPLC system and a Sciex API 5000 (Applied Biosystems, Foster City, CA) mass spectrometer in the Multiple Reaction Monitoring (MRM) scan mode with electrospray ionization (ESI). The mobile phase consisted of water (A) and acetonitrile (B) both containing 0.1% formic acid. The chromatography was performed on

Phenomenex Kinetex XB-C18 (2.0 x 50 mm, 5.0 μM) column using a gradient elution method (2% B from 0.0 to 0.3 min, followed by a linear increase to 50% B over 2.7 min and subsequently 95 % B for 0.1 min, and held at 95% B for an additional .0.9 min before returning back to 2% B) at a flow rate of 0.6 mL/min. The following transitions were monitored: *m/z* 152.1→110.0 (acetaminophen – CYP1A2), *m/z* 870.3→105.1 (6α-hydroxy-taxol – CYP2C8), *m/z* 312.1→230.0 (4-hydroxy-diclofenac – CYP2C9), *m/z* 235.3→150.2 (4-hydroxy-*S*-mephenytoin – CYP2C19), *m/z* 258.2→157.1 (dextrorphan – CYP2D6), *m/z* 342.2→297.1 (1-hydroxy-midazolam – CYP3A), and *m/z* 253.1→182.2 for phenytoin (internal standard). Data were processed using Analyst software with probe metabolite to internal standard peak area ratios electronically exported into Excel 2000 (Microsoft Corp., Seattle, WA) format.

Definitive CYP Inhibition Assay. Studies were conducted in human liver microsomes where each reaction consisted of a single probe co-incubated with JNJ-54166060 at test concentrations ranging from 90 – 0.09 μM . The following probes were incubated at ~ their K_M concentrations: phenacetin (CYP1A2 – 80 μM), coumarin (CYP2A6 – 2 μM), bupropion (CYP2B6 – 20 μM), amodiaquine (CYP2C8 – 2 μM), tolbutamide (CYP2C9 – 100 μM), diclofenac (CYP2C9 – 5 μM), *S*-mephenytoin (CYP2C19 – 30 μM), dextromethorphan (CYP2D6 – 3 μM), chlorzoxazone (CYP2E1 – 45 μM), testosterone (CYP3A – 25 μM), midazolam (CYP3A – 2 μM), and nifedipine (CYP3A – 10 μM). Incubation conditions and LC/MS/MS methodology were optimized for the product formation and detection, respectively, of each probe metabolite, and IC_{50} values were determined relative to activity observed in vehicle treated incubations.

CYP3A Time Dependent Inhibition (TDI). DMSO stocks were prepared for test compounds (10 mM), the assay positive control troleandomycin (5 mM) and the assay negative control

ketoconazole (0.3 mM) and diluted 25-fold in a mixture of acetonitrile:water (30/70, v/v). Human liver microsomes at 0.3 mg/mL in 100 mM potassium phosphate buffer (pH 7.4) supplemented with 3 mM $MgCl_2$ and 1 mM NADPH in a total volume of 0.1 mL were pre-incubated for 30 minutes at 37°C in the absence or presence of various concentrations of test compounds, positive or negative control. Following a 30-minute pre-incubation, blank liver microsomes were also spiked with test compounds, positive or negative controls. All samples were then mixed with 0.1 mL of 100 mM potassium phosphate buffer (pH 7.4) containing 3 mM $MgCl_2$, 1 mM NADPH and 50 μM testosterone and the secondary incubations were carried out for 10 min at 37 °C. The final inhibitor concentrations in secondary incubations were as follows: 0.04, 0.12, 0.37, 1.1, 3.3 and 10 μM for test compounds; 0.02, 0.06, 0.19, 0.6, 1.7 and 5 μM for troleandomycin; and 0.0012, 0.0037, 0.01, 0.03, 0.1 and 0.3 μM for ketoconazole. The reaction was terminated by the addition of 0.2 mL of acetonitrile containing the internal standard (0.1 μg/mL phenytoin). The samples were vortexed and centrifuged at 3,200 rpm for 10 min. The supernatant (0.2 mL) was removed and mixed with 0.1 mL of water in a fresh 96-well plate. A 20-μL aliquot was analyzed for probe metabolite formation using Shimadzu SCL-10A HPLC and a Sciex API 4000 Q-Trap (Applied Biosystems, Foster City, CA) mass spectrometer in the Multiple Reaction Monitoring (MRM) scan mode with electrospray ionization (ESI). The mobile phase consisted of water (A) and acetonitrile (B) both containing 0.1% formic acid. The chromatography was performed on an Agilent Zorbax SB-phenyl (2.1 × 50 mm, 5 μm) column using a gradient elution method (10% B from 0.1 to 0.3 min, then to 95% B over 1.4 min and held at 95% B for an additional 1.0 min before returning back to 10% B) at a flow rate of 0.8 mL/min. The transitions monitored were *m/z* 305→269 for 6β-hydroxy-testosterone and *m/z*

253.1→182.2 for phenytoin (internal standard). Data were processed using Analyst software and included 6β-hydroxy-testosterone to internal standard peak area ratios electronically exported into Excel 2000 (Microsoft Corp., Seattle, WA) format. The concentration required for 50% inhibition of CYP3A4 activity (IC_{50}) was calculated using Janssen proprietary software from the percent CYP3A4 activity remaining after compound incubation at various concentrations relative to vehicle, based on the 6β-hydroxy-testosterone to internal standard peak ratio. The fold shift in the IC_{50} was calculated as a ratio of the IC_{50} values without and with pre-incubation. A greater than 2-fold shift in the IC_{50} value as a result of pre-incubation was considered a threshold for time-dependent inhibition.

Metabolite Identification in Liver Microsomes. From a 10 mM DMSO stock solution, test compound (10 μM) was incubated in liver microsomes (1 mg/mL protein concentration) from rat and human in 100 mM potassium phosphate buffer (pH 7.4) fortified with 25 μg/mL alamethicin, 3 mM MgCl2, 1 mM NADPH, 5 mM GSH, and 3 mM UDPGA. The reaction was allowed for 60 min at 37º C before terminated with the addition of 1.5 volumes of ice-cold acetonitrile/methanol mixture (3:1, v/v). The samples were centrifuged for 10 min at 2880 *g* to precipitate proteins prior to injecting a 100 μL aliquot onto the LC/MS system. The LC/MS/MS analysis was conducted using Surveyor HPLC system interfaced to a UV detector (214, 254 and 280 nm) and a LTQ-Orbitrap XL high resolution mass spectrometer (Thermo-Finnigan, San Jose, CA). The Fourier Transform Mass Spectrometer (FTMS) of the LTQ-Orbitrap XL was operated in the positive mode set for four scan events. The first scan event, a full scan from 200 – 1000 m/z acquired at a resolution of 15,000, was followed by three data dependent MS2 scan events acquired at a resolution of 7,5000 to aide structural identification of JNJ-54175446 metabolites. Chromatographic separation was achieved on a Zorbax SB-C18 column (4.6 x 150

mm, 3.5 µm particle size) using a gradient elution method (0-5 min, 5% B; 5-47 min, 80% B; 47 - 50 min, 80% B; 50-51 min, 80-98 % B; 51-55 min, 98% B; 55.0 – 55.1 min, 98 – 5% B; and 55.1 – 60 min, 5% B) at a flow rate of 0.3 mL/min. The mobile phase consisted of 0.1% formic acid in water (A) and 0.1% formic acid in acetonitrile (B). The HPLC-MS/MS data was analyzed using Xcalibur MS software (Thermo-Finnigan, San Jose, CA) and Janssen Research & Development internal MS fragmentation prediction software PrISE 2.1.1, developed by Dotmatics Limited (Hill and Mortishire-Smith, 2005, Rapid Commun Mass Spectrom). The assignment and localization of metabolites was determined from the observed molecular weights from full scan mass spectra and through interpretation of fragment ions produced for metabolite relative to unchanged drug from MS/MS spectra.

Single Crystal Growth Experiments. A solubility assessment was carried out on **1** and **31** using twenty three solvents. **1** and **31** were treated with 20 µl of each solvent at RT or 100 µl of solvent at 50 ºC in order to obtain clear solutions. Suspensions were matured between RT and 50 ºC (4 h at each temperature – 8 h cycle) for 3 weeks. Solutions were cooled to 5 ºC and kept at this temperature for 48 h. If no solids were obtained, the solutions were then further cooled to -20 ºC and kept at this temperature for 24 h. Any solutions or slurries obtained at 5 or -20 ºC were then left to evaporate slowly at RT. All experiments were checked regularly for single crystals. Single crystals were obtained from slow evaporation from toluene and DMSO for compound **1** and from acetone and DMSO for compound **31**.

Single Crystal X-Ray Diffraction. Data were collected on a Rigaku Oxford Diffraction Supernova Dual Source, Cu at Zero, Atlas CCD diffractometer equipped with an Oxford Cryosystems Cobra cooling device. Data were collected using CuKα radiation. Structures were typically solved using either the SHELXS programs and refined with the SHELXL program as

part of the Bruker AXS SHELXTL suite (V6.10). Unless otherwise stated, hydrogen atoms attached to carbon were placed geometrically and allowed to refine with a riding isotropic displacement parameter. Hydrogen atoms attached to a heteroatom were located in a difference Fourier synthesis and were allowed to refine freely with an isotropic displacement parameter.

Pharmacokinetic Studies. Single dose pharmacokinetic studies in preclinical species (male Balb/c mice, Sprague Dawley rats, beagle dogs, or cynomolgus monkeys) were conducted following iv (1 mg/kg) and po (5 mg/kg) administration as a solution in 20% hydroxypropyl-β-cyclodextrin (HP-β-CD). Blood was sampled at predose and at 0.033 (iv), 0.083 (iv), 0.25, 0.5, 1, 2, 4, 6, 8, and 24 h postdose. In dogs, instead of 6 and 8 h time points blood was drawn at 7 h. Plasma concentrations were quantitated by LCMS/MS. Pharmacokinetic parameters were derived from noncompartmental analysis of the plasma concentration vs time data using WinNonlin software (Pharsight, Palo Alto, CA).

1 and 4-Day Repeat Dose Oral Toxicology Studies. For the single dose study toxicology group animals were administered **1** at oral doses of 125, 250, 500, and 1000 mg/kg/day with necropsy performed on day 2. For the repeat dose toxicology group animals were administered **1** at oral doses of 62.5, 125 or 250 mg/kg/day for 4 days, with necropsy performed on day five. The tissues from control and treated groups were embedded in paraffin, processed into slides by sectioning at 4μm, stained with hematoxylin and eosin, and examined microscopically.

ASSOCIATED CONTENT

Supporting Information. Metabolite identification results, csv files, and crystallography reports.

AUTHOR INFORMATION

Corresponding Author

*Email: dswanso1@its.jnj.com. Tel: 1-858-320-3306

Author Contributions

The manuscript was written through contributions of all authors.

Notes

The authors declare no competing financial interest.

ABBREVIATIONS USED

SAR, structure−activity relationship; MW, molecular weight; po, per os; CL, clearance; Vss, volume of distribution at steady state; t1/2, half life; F, bioavailability; RLM, rat liver microsome; HLM, human liver microsome; CYP, cytochrome P450; RO, receptor occupancy; PPB, plasma protein binding; PK, pharmacokinetics; ADME, absorption distribution metabolism and excretion; BnBr, benzyl bromide; $NaBH_4$, sodium borohydride; HPLC, high performance liquid chromatography; hERG, human Ether-à-go-go-Related Gene; MET ID, metabolism identification; QD, quaque die (once a day); CNS, central nervous system; LC-MS, liquid chromatography-mass spectrometry;

Acknowledgments

The authors would like to thank Heather Mcallister, Khoa Tran, Sandrine Jolly and Laurence Queguiner for analytical support and Michael Ameriks for input and suggestions.

References

1. Bhattacharya, A.; Biber, K. The microglial ATP-gated ion channel P2X7 as a CNS drug target. *Glia* **2016**, *64*, 1772-1787.

2. Collo, G.; Neidhart, S.; Kawashima, E.; Kosco-Vilbois, M.; North, R. A.; Buell, G. Tissue distribution of the P2X7 receptor. *Neuropharmacology* **1997**, *36*, 1277-1283.

3. Solle, M.; Labasi, J.; Perregaux, D. G.; Stam, E.; Petrushova, N.; Koller, B. H.; Griffiths, R. J.; Gabel, C. A. Altered cytokine production in mice lacking P2X(7) receptors. *J. Biol. Chem.* **2001**, *276*, 125-132.

4. Chataigneau, T.; Lemoine, D.; Grutter, T. Exploring the ATP-binding site of P2X receptors. *Front. Cell Neurosci.* **2013**, *7*, 273.

5. Ando, R. D.; Sperlagh, B. The role of glutamate release mediated by extrasynaptic P2X7 receptors in animal models of neuropathic pain. *Brain. Res. Bull.* **2013**, *93*, 80-85.

6. Wang, C. M.; Chang, Y. Y.; Kuo, J. S.; Sun, S. H. Activation of P2X(7) receptors induced [(3)H]GABA release from the RBA-2 type-2 astrocyte cell line through a Cl(-)/HCO(3)(-)-dependent mechanism. *Glia* **2002**, *37*, 8-18.

7. Clark, A. K.; Staniland, A. A.; Marchand, F.; Kaan, T. K.; McMahon, S. B.; Malcangio, M. P2X7-dependent release of interleukin-1beta and nociception in the spinal cord following lipopolysaccharide. *J. Neurosci.* **2010**, *30*, 573-582.

8. Shiratori, M.; Tozaki-Saitoh, H.; Yoshitake, M.; Tsuda, M.; Inoue, K. P2X7 receptor activation induces CXCL2 production in microglia through NFAT and PKC/MAPK pathways. *J. Neurochem.* **2010**, *114*, 810-819.

9. Stock, T. C.; Bloom, B. J.; Wei, N.; Ishaq, S.; Park, W.; Wang, X.; Gupta, P.; Mebus, C. A. Efficacy and safety of CE-224,535, an antagonist of P2X7 receptor, in treatment of patients

with rheumatoid arthritis inadequately controlled by methotrexate. *J. Rheumatol.* **2012**, *39*, 720-727.

10. Eser, A.; Colombel, J. F.; Rutgeerts, P.; Vermeire, S.; Vogelsang, H.; Braddock, M.; Persson, T.; Reinisch, W. Safety and efficacy of an oral inhibitor of the purinergic receptor P2X7 in adult patients with moderately to severely active crohn's disease: A randomized placebo-controlled, double-blind, phase IIa study. *Inflamm. Bowel Dis.* **2015**, *21*, 2247-2253.

11. Ali, Z.; Laurijssens, B.; Ostenfeld, T.; McHugh, S.; Stylianou, A.; Scott-Stevens, P.; Hosking, L.; Dewit, O.; Richardson, J. C.; Chen, C. Pharmacokinetic and pharmacodynamic profiling of a P2X7 receptor allosteric modulator GSK1482160 in healthy human subjects. *Br. J. Clin. Pharmacol.* **2013**, *75*, 197-207.

12. Iwata, M.; Ota, K. T.; Li, X. Y.; Sakaue, F.; Li, N.; Dutheil, S.; Banasr, M.; Duric, V.; Yamanashi, T.; Kaneko, K.; Rasmussen, K.; Glasebrook, A.; Koester, A.; Song, D.; Jones, K. A.; Zorn, S.; Smagin, G.; Duman, R. S. Psychological stress activates the inflammasome via release of adenosine triphosphate and stimulation of the purinergic type 2X7 receptor. *Biol. Psychiatry* **2016**, *80*, 12-22.

13. Basso, A. M.; Bratcher, N. A.; Harris, R. R.; Jarvis, M. F.; Decker, M. W.; Rueter, L. E. Behavioral profile of P2X7 receptor knockout mice in animal models of depression and anxiety: relevance for neuropsychiatric disorders. *Behav. Brain Res.* **2009**, *198*, 83-90.

14. Savall, B. M.; Wu, D.; De Angelis, M.; Carruthers, N. I.; Ao, H.; Wang, Q.; Lord, B.; Bhattacharya, A.; Letavic, M. A. Synthesis, SAR, and pharmacological characterization of brain penetrant P2X7 receptor antagonists. *ACS Med. Chem. Lett.* **2015**, *6*, 671-676.

15. Rudolph, D. A.; Alcazar, J.; Ameriks, M. K.; Anton, A. B.; Ao, H.; Bonaventure, P.; Carruthers, N. I.; Chrovian, C. C.; De Angelis, M.; Lord, B.; Rech, J. C.; Wang, Q.;

Bhattacharya, A.; Andres, J. I.; Letavic, M. A. Novel methyl substituted 1-(5,6-dihydro-[1,2,4]triazolo[4,3-a]pyrazin-7(8H)-yl)methanones are P2X7 antagonists. *Bioorg. Med. Chem. Lett.* **2015**, *25*, 3157-3163.

16. Dean, D., K. ; Munoz-Muriedas, J.; Sime, M.; Steadman, J.; A., G.; Thewlis, R. A. E.; Trani, G.; Walter, D. S. *PCT Int. Appl.* **2010**, WO 2010125102.

17. Ameriks, M. K.; Ao, H.; Carruthers, N. I.; Lord, B.; Ravula, S.; Rech, J. C.; Savall, B. M.; Wall, J. L.; Wang, Q.; Bhattacharya, A.; Letavic, M. A. Preclinical characterization of substituted 6,7-dihydro-[1,2,4]triazolo[4,3-a]pyrazin-8(5H)-one P2X7 receptor antagonists. *Bioorg. Med. Chem. Lett.* **2016**, *26*, 257-261.

18. Ziff, J.; Rudolph, D. A.; Stenne, B.; Koudriakova, T.; Lord, B.; Bonaventure, P.; Lovenberg, T. W.; Carruthers, N. I.; Bhattacharya, A.; Letavic, M. A.; Shireman, B. T. Substituted 5,6-(dihydropyrido[3,4-d]pyrimidin-7(8H)-yl)-methanones as P2X7 antagonists. *ACS Chem. Neurosci.* **2016**, *7*, 498-504.

19. Chrovian, C. C.; Soyode-Johnson, A.; Ao, H.; Bacani, G. M.; Carruthers, N. I.; Lord, B.; Nguyen, L.; Rech, J. C.; Wang, Q.; Bhattacharya, A.; Letavic, M. A. Novel phenyl-substituted 5,6-dihydro-[1,2,4]triazolo[4,3-a]pyrazine P2X7 antagonists with robust target engagement in rat brain. *ACS Chem. Neurosci.* **2016**, *7*, 490-497.

20. Rech, J. C.; Bhattacharya, A.; Letavic, M. A.; Savall, B. M. The evolution of P2X7 antagonists with a focus on CNS indications. *Bioorg. Med. Chem. Lett.* **2016**, *26*, 3838-3845.

21. Alcasar, J.; Ignacio, J.; Chrovian, C. C.; Angelis, M. D.; Dvorak, C.; Gelin, C.; Letavic, M.; Savall, B. M.; Soyode-Johnson, A.; Stenne, B.; Swanson, D. M. *PCT Int. Appl.* **2014**, US 20140275015

22. Altman, R. A.; Buchwald, S. L. 4,7-Dimethoxy-1,10-phenanthroline: an excellent ligand for the Cu-catalyzed N-arylation of imidazoles. *Org. Lett.* **2006**, *8*, 2779-2782.

23. Comins, D. L.; Abdullah, A. H. Regioselective addition of Grignard reagents to 1-acylpyridinium salts. A convenient method for the synthesis of 4-alkyl(aryl)pyridines. *J. Org. Chem.* **1982**, *47*, 4315.

24. Flack, H. D. On enantiomorph-polarity estimation. *Acta Crystallogr. A* **1983**, A39, 876-881.

25. Lord, B.; Ameriks, M. K.; Wang, Q.; Fourgeaud, L.; Vliegen, M.; Verluyten, W.; Haspeslagh, P.; Carruthers, N. I.; Lovenberg, T. W.; Bonaventure, P.; Letavic, M. A.; Bhattacharya, A. A novel radioligand for the ATP-gated ion channel P2X7: [H] JNJ-54232334. *Eur. J. Pharmacol.* **2015**, *765*, 551-559.

26. Mastey, V.; Panneton, A. C.; Donati, F.; Varin, F. Determination of midazolam and two of its metabolites in human plasma by high-performance liquid chromatography. *J Chromatogr B. Biomed. Appl.* **1994**, *655*, 305-310.

27. Yuan, R.; Madani, S.; Wei, X. X.; Reynolds, K.; Huang, S. M. Evaluation of cytochrome P450 probe substrates commonly used by the pharmaceutical industry to study in vitro drug interactions. *Drug Metab. Dispos.* **2002**, *30*, 1311-1319.

28. van Breemen, R. B.; Li, Y. Caco-2 cell permeability assays to measure drug absorption. *Expert Opin. Drug Metab. Toxicol.* **2005**, *1*, 175-185.

29. Houston, J. B.; Galetin, A. Methods for predicting in vivo pharmacokinetics using data from in vitro assays. *Curr. Drug Metab.* **2008**, *9*, 940-951.

Table of Contents Graphic

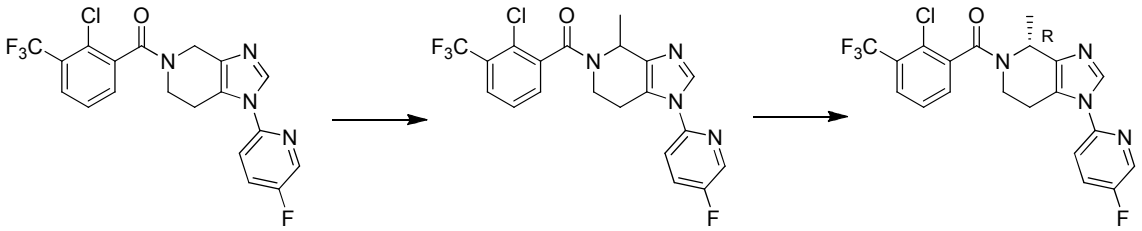

14
hP2X7 IC_{50} = 28 nM
rP2X7 IC_{50} = 2476 nM
HLM/RLM = 0.84/0.87

27
hP2X7 IC_{50} = 14 nM
rP2X7 IC_{50} = 592 nM
HLM/RLM = <0.3/0.52

1
hP2X7 IC_{50}= 4 nM
rP2X7 IC_{50}= 115 nM
HLM/RLM = 0.35/0.64

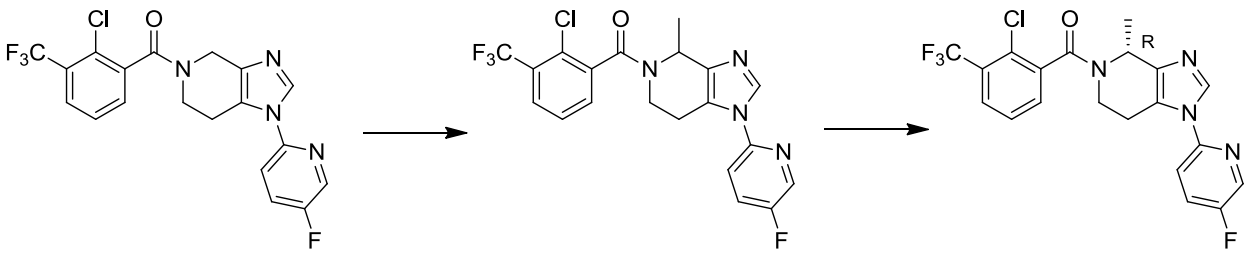

14
hP2X7 IC_{50} = 28 nM
rP2X7 IC_{50} = 2476 nM
HLM/RLM = 0.84/0.87

27
hP2X7 IC_{50} = 14 nM
rP2X7 IC_{50} = 592 nM
HLM/RLM = <0.3/0.52

1 (JNJ 54166060)
hP2X7 IC_{50} = 4 nM
rP2X7 IC_{50} = 115 nM
HLM/RLM = 0.35/0.64

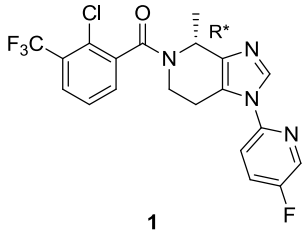

1
(JNJ 54166060)

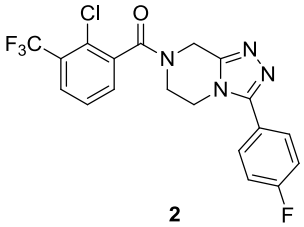

2
hP2X7 IC_{50} = 14 nM
rP2X7 IC_{50} = 6400 nM

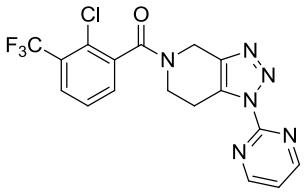

3
hP2X7 IC_{50} = 4 nM
rP2X7 IC_{50} = 7 nM

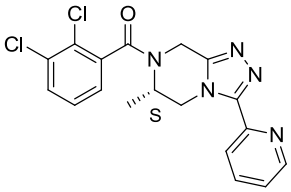

4
hP2X7 IC_{50} = 8 nM
rP2X7 IC_{50} = 8 nM

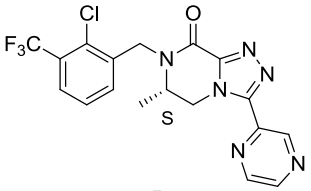

5
hP2X7 IC_{50} = 0.7 nM
rP2X7 IC_{50} = 79 nM

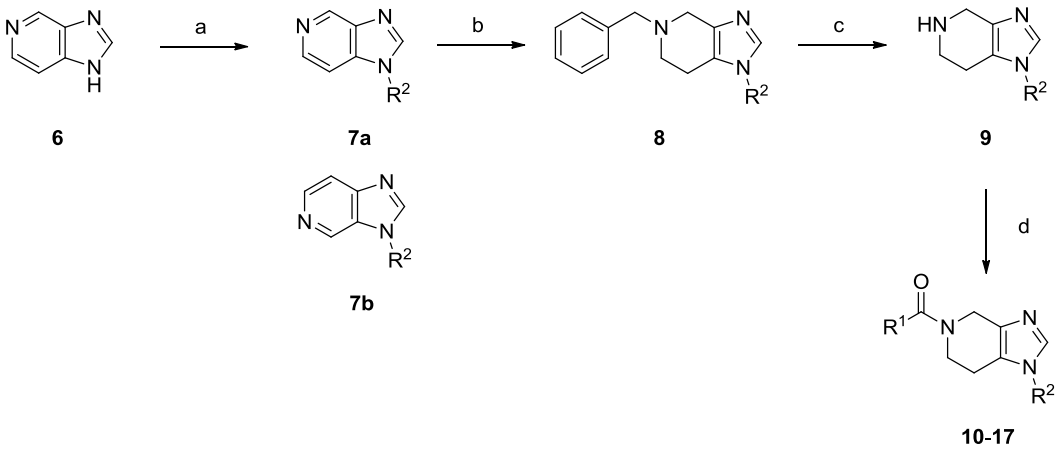

Reagents & Conditions: a) R^2-X, Cu_2O, 8-OH quinoline, Cs_2CO_3, DMSO, microwave, 1 h, 140 °C, 17-40% b) BnBr, $NaBH_4$, DCM, MeOH, rt, 68-87% c) H_2, EtOH, Pd/C, rt, 24 h, 75-83% d) R^1COOH, HATU, Et_3N, DMF, rt, 22-96%

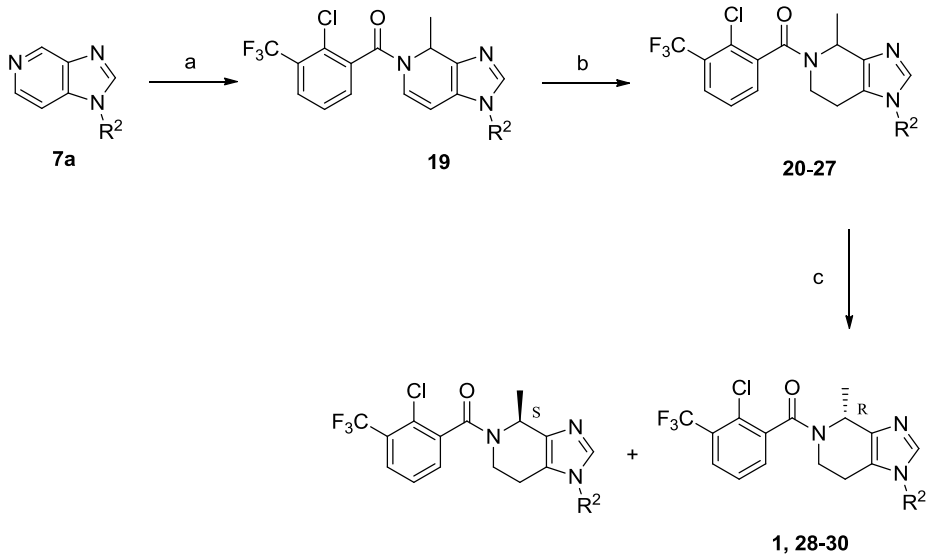

Reagents & Conditions: a) 2-Cl-3-CF_3PhCOCl (**18**), MeMgBr, THF, rt, 3 h, 33-54% b) H_2, EtOH, Pd/C, 24 h, 20-62% c) SFC chiral chromatography, 40-42%

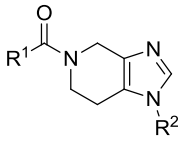

Compd	R^1	R^2	hP2X7 IC_{50} (nM)[a]	rP2X7 IC_{50} (nM)[b]	HLM/ RLM[c]
10	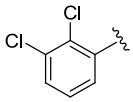		89	4006	0.93/>0.92
11	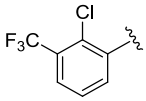		12	2909	0.94/0.89
12	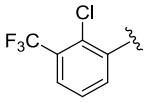		4	609	0.91/>0.92
13	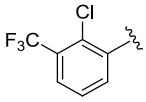		9	1782	0.9/0.87
14	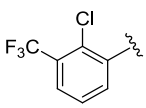	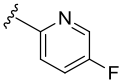	28	2476	0.84/0.87
15	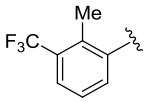	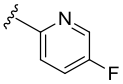	114	4872	--
16	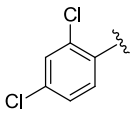	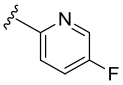	880	>10,000	--
17	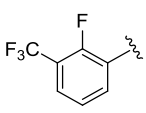	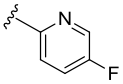	3538	>10,000	--

[a]All compounds were found to be P2X7 antagonists using a human peripheral blood monocyte (HPBMC) assay prior to testing in FLIPR for confirmation of activity and IC_{50} determination. The protocols for the HPBMC and FLIPR assays can be found in the Experimental Section. Human FLIPR pIC_{50} measured in a Ca^{2+} flux assay. [b]Rat FLIPR measured in a Ca^{2+} flux assay. [c]Stability in rat and human liver microsomes as measured by extraction ratio(s). Primary assays run in triplicate with the mean value reported. Standard deviation in all cases was less than two-fold.

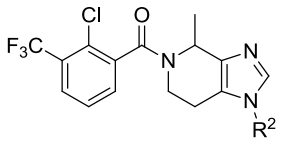

Compd	R^2	hP2X7 IC_{50} (nM)[a]	rP2X7 IC_{50} (nM)[b]	HLM/ RLM[c]
20		5	766	0.75/0.73
21	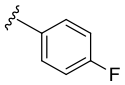	78	1182	0.32/0.59
22		30	113	0.79/0.80
23	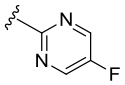	10	3828	<0.3/0.54
24		77	1225	0.77/0.84
25		34	295	0.74/0.89
26		9	2319	0.81/0.81
27	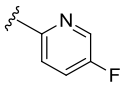	14	592	<0.3/0.52

[a]Human FLIPR pIC_{50} measured in a Ca^{2+} flux assay. [b]Rat FLIPR measured in a Ca^{2+} flux assay. [c]Stability in rat and human liver microsomes reported as hepatic extraction ratio(s). Primary assays have been run in triplicate with the mean value reported. Standard deviation in all cases was less than two-fold.

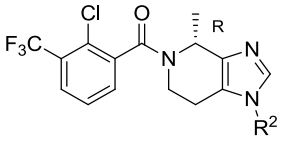

Compd	R^2	hP2X7 IC_{50} (nM)[a]	rP2X7 IC_{50} (nM)[b]	mP2X7 IC_{50} (nM)[c]	hP2X7 K_i (nM)[d]
28	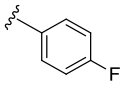	67	303	45	40
29		15	116	20	32
1	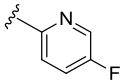	4	115	72	7
30	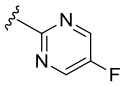	34	300	38	22

[a]Human FLIPR pIC_{50} measured in a Ca^{2+} flux assay. [b]Rat FLIPR measured in a Ca^{2+} flux assay. [c]Mouse FLIPR measured in a Ca^{2+} flus assay. [d]Human K_i measured with [^{3}H]-**5** as the binding ligand. All assay data has been run in triplicate with the mean value reported. Standard deviation in all cases was less than two-fold.

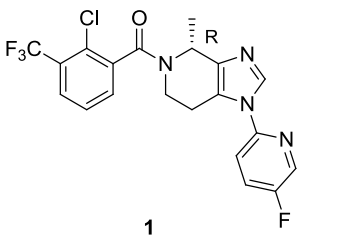

1

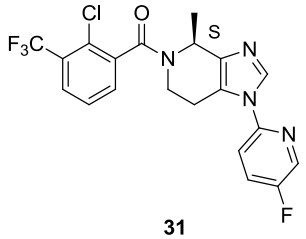

31

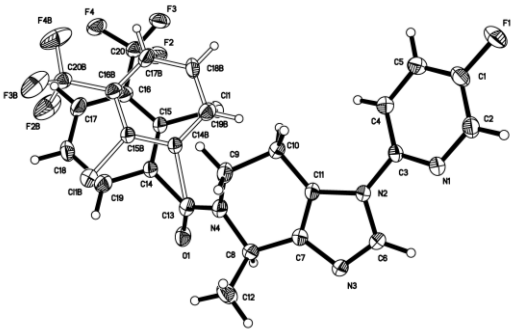

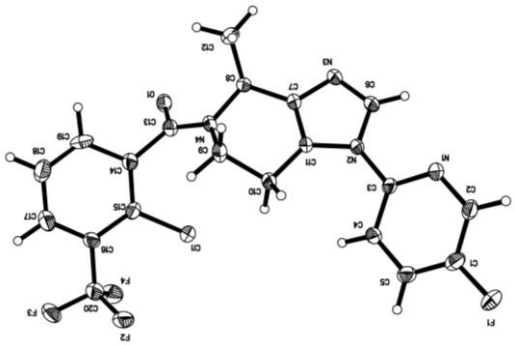

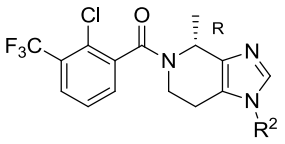

Compd	R^2	HLM/ RLM[a]	h/r PPB[b]	CYPs IC_{50} (μM)[c]	hERG dofet IC_{50} (μM)[d]	Solub. pH2/pH7 (μM)
28	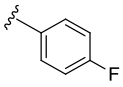	0.36/0.40	96/97.5	> 10	> 10	165/14
29	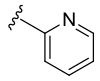	0.63/0.85	95.3/97.4	> 10	> 10	>400/20
1	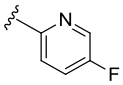	0.35/0.64	94.5/94.9	> 10	> 10	>400/29
30	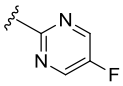	<0.3/0.73	95.2/96.2	2C19 = 7.8	> 10	>400/4

[a]Stability in rat and human liver microsomes reported as hepatic ratio(s). [b]Human and rat plasma protein binding reported as % bound. [c]Screening CYP inhibition data obtained from human liver microsomes. [d]hERG IC_{50} as measured in an [^{3}H]astemizole competition binding assay in HEK-293 cells expressing the hERG channel.

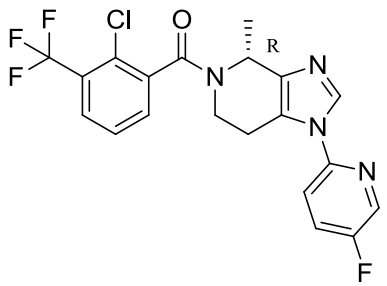

1

h/r/m P2X7 IC_{50} (nM) = 4/115/72

h/r P2X7 K_i (nM) = 7/8

h/m P2X7 Whole Blood IC_{50} (nM) = 92/160

LM h/r/m/d/mk = 0.35/0.67/0.56/0.33/0.41

CYP IC_{50} (μM) all > 10

h/r/m PPB (%) = 94.5/94.9/95.5

rBB = 98.5

hERG IC_{50} (dof. μM) >10

Caco-2 BA/AB = 35/65

solubility pH2/pH7 (μM) = >400/29

Cerep panel = clean @ 1μM

Upstate panel = clean @ 1 μM

CYP phenotyping = CYP3A4

TDI = clean below 10 μM

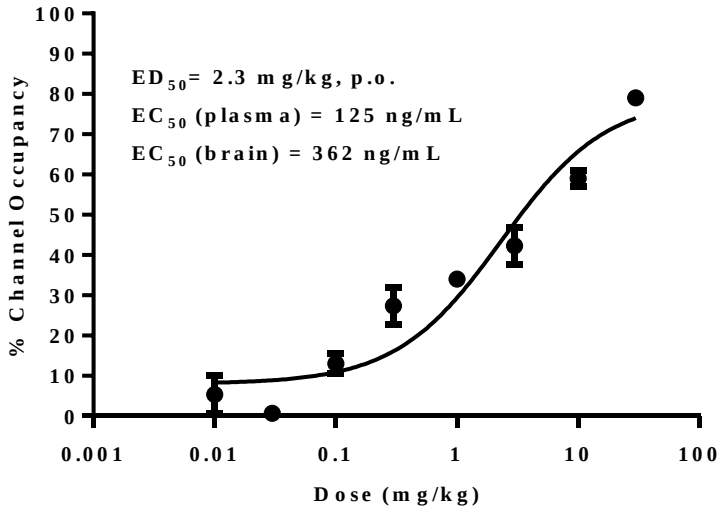
ED50= 2.3 mg/kg, p.o.
EC50 (plasma) = 125 ng/mL
EC50 (brain) = 362 ng/mL
% Channel Occupancy
100
90
80
70
60
50
40
30
20
10
0
0.001
0.01
0.1
1
10
100
Dose (mg/kg)

	In vitro from LMs	IV			PO		
	CL[a] (ml/min/kg)	CL[a] (ml/min/kg)	Vss[b] (L/kg)	$t_{1/2}$[c] (hr)	C_{max}[d] (ng/mL)	t_{max}[e] (hr)	F (%)
Rat	36.8	30	3.8	1.7	375	1	55
Dog	10.3	5.5	3.6	11.9	1249	0.5	>100
Monkey	18.2	14	2.1	4.2	389	2.3	54
Human (predicted)	7.3	2.8	2.0	8.3	--	--	85

[a] = Clearance, [b] = Volume of Distribution at steady state [c] = IV half live, [d] = Maximum concentration [e] = Time of maximum concentration

1

Rat PO SD Toleration

Vehicle: 0.5% HPMC Suspension (10 mL/kg)

20% HPbCD Solution (10 mL/kg)

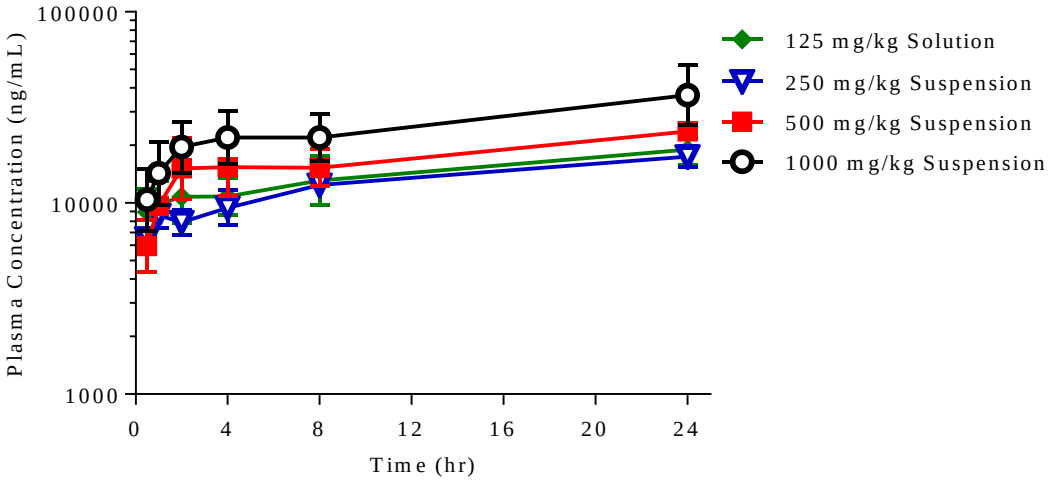

1

Rat PO RD Toleration

Vehicle: 20%HPbCD (10 mL/kg) for 62.5 and 125 mg/kg doses

0.5% HPMC (10 mL/kg) for 250 mg/kg dose

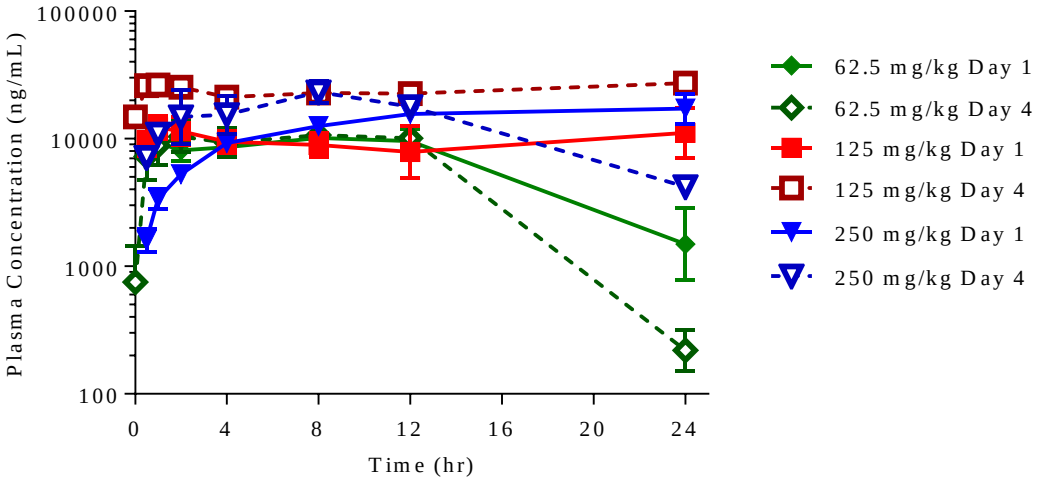

1			Ketoconazole (CYP3A4 positive control)		
Concentration (μM)	1-OH-Midazolam % inhibition	4-OH-Midazolam % inhibition	Concentration (μM)	1-OH-Midazolam % inhibition	4-OH-Midazolam % inhibition
0.313	20	0.1	0.005	34	37
0.625	29	-5	0.01	53	57
1.25	41	-10	0.02	70	74
2.5	52	-13	0.04	82	85
5	63	-13	0.08	90	92
10	74	-4	0.16	94	95